EUR 2553.e

EUROPEAN ATOMIC ENERGY COMMUNITY - EURATOM

DYNAMICS AND CONTROL OF THE FAST PULSED REACTOR "SORA"

by

H. WUNDT and G. P. CALIGIURI

1965

Joint Nuclear Research Center
Ispra Establishment - Italy

Reactor Physics Department
Research Reactors Service
and
Scientific Data Processing Center - CETIS

LEGAL NOTICE

This report is on sale at the addresses listed on cover page 4

at the price of	FF 15	FB 150	DM 12	Lit. 1870	Fl. 11

When ordering, please quote the EUR number and the title, which are indicated on the cover of each report.

Printed by L. Vanmelle, S.A. - Gent
Brussels, November 1965

EUR 2553.e

DYNAMICS AND CONTROL OF THE FAST PULSED REACTOR « SORA » by G.P. CALIGIURI and H. WUNDT

European Atomic Energy Community - EURATOM
Joint Nuclear Research Center - Ispra Establishment (Italy)
Reactor Physics Department - Research Reactors Service and
Scientific Data Processing Center - CETIS
Brussels, November 1965 - 102 Pages - 10 Figures - FB 150

A detailed description of the dynamic behaviour of the reactivity-pulsed research reactor SORA is presented, based on results of a simulation on an analog computer. The periodically pulsed state is treated, as well as disturbances from it. Temperature feedback is considered. A suitable control is designed to keep the reactor stable though it becomes prompt-supercritical fifty times per second.

The simulation itself required new combined digital-analog techniques which are equally described.

EUR 2553.e

DYNAMICS AND CONTROL OF THE FAST PULSED REACTOR « SORA » by G.P. CALIGIURI and H. WUNDT

European Atomic Energy Community - EURATOM
Joint Nuclear Research Center - Ispra Establishment (Italy)
Reactor Physics Department - Research Reactors Service and
Scientific Data Processing Center - CETIS
Brussels, November 1965 - 102 Pages - 10 Figures - FB 150

A detailed description of the dynamic behaviour of the reactivity-pulsed research reactor SORA is presented, based on results of a simulation on an analog computer. The periodically pulsed state is treated, as well as disturbances from it. Temperature feedback is considered. A suitable control is designed to keep the reactor stable though it becomes prompt-supercritical fifty times per second.

The simulation itself required new combined digital-analog techniques which are equally described.

EUR 2553.e

DYNAMICS AND CONTROL OF THE FAST PULSED REACTOR « SORA » by G.P. CALIGIURI and H. WUNDT

European Atomic Energy Community - EURATOM
Joint Nuclear Research Center - Ispra Establishment (Italy)
Reactor Physics Department - Research Reactors Service and
Scientific Data Processing Center - CETIS
Brussels, November 1965 - 102 Pages - 10 Figures - FB 150

A detailed description of the dynamic behaviour of the reactivity-pulsed research reactor SORA is presented, based on results of a simulation on an analog computer. The periodically pulsed state is treated, as well as disturbances from it. Temperature feedback is considered. A suitable control is designed to keep the reactor stable though it becomes prompt-supercritical fifty times per second.

The simulation itself required new combined digital-analog techniques which are equally described.

EUR 2553.e

EUROPEAN ATOMIC ENERGY COMMUNITY - EURATOM

DYNAMICS AND CONTROL OF THE FAST PULSED REACTOR "SORA"

by

H. WUNDT and G. P. CALIGIURI

1965

Joint Nuclear Research Center
Ispra Establishment - Italy

Reactor Physics Department
Research Reactors Service
and
Scientific Data Processing Center - CETIS

SUMMARY

A detailed description of the dynamic behaviour of the reactivity-pulsed research reactor SORA is presented, based on results of a simulation on an analog computer. The periodically pulsed state is treated, as well as disturbances from it. Temperature feedback is considered. A suitable control is designed to keep the reactor stable though it becomes prompt-supercritical fifty times per second.

The simulation itself required new combined digital-analog techniques which are equally described.

Contents

Contents - continued

Introduction

Since 1962, a fast research reactor has been under design by the Reactor Physics Department of the Joint Nuclear Research Center of Ispra which - though able to operate also under steady conditions - is foreseen to give periodically repeated neutron pulses with very high intensity and short duration.

The use of neutron choppers with the constant neutron flux of a normal reactor means a waste of energy, since only a small time fraction is utilized, with all associated problems of cooling. Another principle is to "chop" not the output of the reactor but already its input, i.e. some quantity like its reactivity. In this case, the mean power of the assembly can be kept relatively modest, while large neutron pulses are produced.

The "SORA" reactor is of the second kind. Its name means "sorgente rapida" (= fast source). The first reactor of pulsed type is the Russian reactor IBR at the Dubna Center. Its mean power is about 3 kW, whereas SORA is being designed for 500 kW mean power. The dynamics and the safe operation of SORA is a problem of central importance, due to lack of experience with a reactor of this type operating at high power.

It is not intended to give a full description of the technical performance here; only those parts will be described which affect the transient behaviour of the reactor in periodically pulsed and disturbed states. We also do not discuss the application or use of the pulsed flux, i.e. the experimental aspects.

Manuscript received on August 13, 1965.

The aim of this paper is to give as completely as possible a picture of the fast transients including kinetics and heat transfer without and, of course, with an appropriate control. To get this information, suitable physical models have been established to describe the different parts. The mathematical equations have been treated on the three PACE 231 R analog computers of our Computing Center CETIS at Ispra.

1. Brief reactor description

In order to obtain pulses as short as possible it is obvious that the neutron lifetime should also be very short. The choice of a fast reactor is therefore imperative.

SORA contains a 5 liter core, 24 cm high and of slightly irregular hexagonal cross section. 107 circular fuel rods form a bundle without spacers. Heat is removed from the core by eutectic NaK flowing between the rods. The rods themselves are made of highly enriched U [1], alloyed with 10 % Mo, radius 7 mm. After a NaK-bond of 0,2 mm, a cladding cylinder follows, made of Incoloy, 0,3 mm thick.

Around the core a reflector for fast neutrons is provided (molybdenum and stainless steel), which is however open at one side of the hexagon. This side is called the "window". The missing part of the reflector is replaced by a block made of beryllium, placed at the end of a propeller arm which rotates with a peripheral velocity of 276 m/sec and a frequency of 50 Hz. Whenever the reflector piece passes along the window, the assembly becomes slightly prompt supercritical, whereas otherwise it is strongly subcritical.

In the reflector, on two sides opposite from the window, two large hydrogeneous scatterers are placed in order to slow down the incoming fast neutrons for experiments with low energy neutrons. Although a boron barrier is placed between the scatterers and the core to prevent as far as possible the return of slow neutrons to the

---

1) The use of PuO_2 fuel is foreseen for later core loadings, but is not considered in this paper.

core, the presence of the moderating material influences somewhat the core neutron spectrum. This feature calls for an energy dependent neutron kinetics as we shall see in detail in paragraph 2.1.

The reactor heat is transferred through a secondary NaK-loop to an open air loop. Transients outside the core, however, need not be considered as a part of the short-range core dynamics, if the nuclear control is properly designed. This will become clear only at the end of this report.

2. Kinetics

The neutron kinetics of a pulsed reactor is more complicated than that of a normal one in which one considers a steady state and then disturbances from it. For a pulsed reactor, the strictly periodic behaviour, which we call "pulsed critical state", corresponds to the stationary state of the normal reactor, whereas the true steady state serves only as the trivial initial condition. In the terminology of normal reactors, the pulsed steady state would correspond already to a special perturbed state, for which, however, a periodicity condition holds which is entirely independent from that for normal criticality. Perturbations from the pulsed state, which are of main interest here, are thus a third stage not encountered in normal systems.

2.1. The basic kinetic equations

The core neutron spectrum has been calculated by Mr. ASAOKA [1] [2] for several configurations and material compositions in a steady state, taking into account the H_2O-scatterers. The whole energy range (10 MeV - 0) has been subdivided into 6 groups and the respective populations computed [1]. It was found that the lower groups with lifetimes larger than the expected power pulse width (about 70 μsec) have non-negligible populations in any case. As a consequence, those neutrons cause fissions only when the flux should have been fallen back to a very small level. A marked deterioration of the output pulse shape has to be feared.

Attempts to consider the slow neutrons as fictitious

---

1) The numerical values used in this paper are not taken from the mentioned reports but have kindly been computed by Mr. ASAOKA on our personal request.

delayed groups led to serious difficulties when defining appropriate "decay constants" and "yields". Such a description proved to be inadequate.

A new foundation of a multigroup kinetics has therefore been undertaken by Mr. SCHWALM [3] by going back to the BOLTZMANN equation. We refer here only the necessary excerpt for an understanding on what will be used for the dynamics.

The neutron energy spectrum is split into an arbitrary number of groups to each of which certain group parameters are attributed. The group angular fluxes f_j are weighted with the adjoint fluxes f_j^+ pertaining to the unperturbed steady state. The new variables

$$n_j(t) = \left(f_j^+,\ f_j(t)\right) , \qquad (2.1.-1)$$

where the bracket means the scalar product (integration over angles and space), depend on time only, so that in fact a multigroup one-point model is considered.

For J groups, Mr. SCHWALM's system reads

$$\dot{n}_j = \frac{(1-\beta)k_j - 1}{l_j} n_j + (1-\beta) \sum_{\substack{j'=1 \\ (j'\neq j)}}^{J} \frac{n_j'}{\Lambda_{j'j}} + \sum_{j'=1}^{j-1} \frac{n_j'}{l_{j'j}} + \sum_{i=1}^{I} \lambda_i C_{i,j}$$

$$j=1,\ldots,J \qquad (2.1.-2)$$

$$\dot{C}_{i,j} = -\lambda_i C_{i,j} + \frac{\beta_i k_j}{l_j} n_j + \beta \sum_{\substack{j'=1 \\ (j'\neq j)}}^{J} \frac{n_j'}{\Lambda_{j'j}} \qquad (2.1.-3)$$

$$i=1,\ldots,I$$
$$j=1,\ldots,J$$

with

β_i = effective (fission spectrum weighted) yield of the i-th delayed group

$$(\beta = \sum_{i=1}^{I} \beta_i),$$

λ_i = decay constant of the i-th group,

$C_{i,j}$ = precursor density of the i-th delayed, j-th energy group.

The meaning of the other coefficients is:

$$k_j = \frac{\chi_j(f_j^+, Pr_j[f_j])}{(f_j^+, K_{d,j}[f_j])} \qquad (2.1.-4)$$

$$\frac{1}{l_j} = \frac{v_j(f_j^+, K_{d,j}[f_j])}{(f_j^+, f_j)} \qquad (2.1.-5)$$

$$\frac{1}{l_{j'j}} = \frac{v_j(f_j^+, K_{in+el,j'j}[f_{j'}])}{(f_j^+, f_{j'})} \qquad (2.1.-6)$$

$$\frac{1}{\Lambda_{j'j}} = \frac{\chi_j v_j(f_j^+, Pr_{j'}[f_{j'}])}{(f_j^+, f_{j'})} \qquad (2.1.-7)$$

with the operators:

$$Pr_j[f_j] = \nu_j \Sigma_{f,j}(\vec{r},t) \cdot \frac{1}{4\pi} \int f_j(\vec{r},\Omega,t)d\Omega \qquad (2.1.-8)$$

production operator

$$K_{d,j}[f_j] = \Omega \cdot \text{grad } f_j + \Sigma_{tot,j}(\vec{r},t) \cdot f_j - K_{in,jj}[f_j] - K_{el,jj}[f_j] \qquad (2.1.-9)$$

destruction operator

$$K_{in,j'j}[f_{j'}] = \Sigma_{in,j'j}(\vec{r},t) \cdot \frac{1}{4\pi} \int f_{j'}(\vec{r},\Omega',t)d\Omega' \qquad (2.1.-10)$$

inelastic scattering from group j' to group j

$$K_{el,j'j}[f_{j'}] = \int \Sigma_{el,j'j}(\vec{r},\Omega' \rightarrow \Omega,t) \cdot f_{j'}(\vec{r},\Omega',t)d\Omega' \qquad (2.1.-11)$$

elastic scattering from group j' to group j and from angle Ω' to angle Ω

and

χ_j = integrated fission spectrum over energy domain j,

v_j = mean neutron velocity in group j,

ν_j = neutrons released per fission in group j.

From these definitions, it can be seen that

k_j is a multiplication factor indicating how many neutrons are produced in group j by a neutron from the same group j,

l_j is the mean lifetime of a neutron in group j which does not leave the group,

$l_{j'j}$ is the mean lifetime of a neutron from group j' appearing finally in group j, or the slowing down time from group j' to group j,

$\Lambda_{j',j}$ is the mean generation time giving the mean time elapsing for the production of a neutron in group j caused by a death in group j'. Correspondingly, $\Lambda_{jj} = l_j/k_j$ indicates the time for a neutron to be produced by a neutron of the same group j.

All these coefficients can, in principle, be calculated by an S_n-code. Since the adjoint flux f^+ is taken for a reference stationary state, the system holds in a "vicinity" of this stationary state only.

Though a 6-group stationary calculation by Mr. ASAOKA [1]) was available from which the coefficients could have been taken, the number of energy groups was reduced to J = 3 in view of the analog treatment, with the following subdivision:

1. group: 10 MeV - 0,454 keV
2. group: 0,454 keV - 0,414 eV
3. group: 0,414 eV - thermal

The odd figures come from the limits in the cross section library. The advantage of the chosen subdivision is that the first group contains the whole fission spectrum. All neutrons are born in this group only ($\chi_1 = 1$, $\chi_2 = \chi_3 = 0$). Consequently, the multiplication factors k_2 and k_3 are both zero; but k_1 will be less than unity for a critical state because of the contributions from the other groups. In addition, the inverse generation times $1/\Lambda_{j',j}$ of the last two groups all vanish.

The third group contains the slow neutrons which preferentially come from the H_2O-scatterer.

---

1) see footnote on p. 9.

It is further assumed that no direct scattering from group 1 to group 3 exists ($1/l_{13} = 0$).

One observes that the equations for $C_{i,2}$ and $C_{i,3}$ contain no source; therefore those precursors immediately die out, and C_{i1} can be called C_i.

If we label $\Lambda_1 \equiv l_1/k_1$, and $\Lambda_2 \equiv \Lambda_{21}$, $\Lambda_3 \equiv \Lambda_{31}$, for brevity, the system reads:

$$\dot{n}_1 = \left[1 - \beta - \frac{1}{k_1}\right]\frac{n_1}{\Lambda_1} + (1-\beta)\left[\frac{n_2}{\Lambda_2} + \frac{n_3}{\Lambda_3}\right] + \sum_{i=1}^{6} \lambda_i C_i \qquad (2.1.-12)$$

$$\dot{n}_2 = -\frac{n_2}{l_2} + \frac{n_1}{l_{12}} \qquad (2.1.-13)$$

$$\dot{n}_3 = -\frac{n_3}{l_3} + \frac{n_2}{l_{23}} \qquad (2.1.-14)$$

$$\dot{C}_i = -\lambda_i C_i + \beta_i\left[\frac{n_1}{\Lambda_1} + \frac{n_2}{\Lambda_2} + \frac{n_3}{\Lambda_3}\right] \qquad i=1,\ldots,6. \qquad (2.1.-15)$$

For convenience, we define dimensionless variables

$$\varphi_j(t) = \frac{n_j(t)}{n_1^o} \qquad (2.1.-16)$$

and

$$c_i(t) = \frac{C_i(t)}{n_1^o}\ , \qquad (2.1.-17)$$

i.e. all variables are normalized to the initial value of the first group flux.

The reduced system looks exactly like (2.1.-12) to (2.1.-15) when writing φ_j instead of n_j and c_l instead of C_l, but the initial conditions are

$$\left.\begin{aligned} \varphi_1^o &= 1 , \qquad \varphi_2^o = \frac{l_2}{l_{12}^o} , \qquad \varphi_3^o = \frac{l_2}{l_{12}^o} \cdot \frac{l_3}{l_{23}} \\ c_l^o &= \frac{\beta_l}{\lambda_l} \sum_{j=1}^{3} \frac{\varphi_j^o}{\Lambda_j} \qquad\qquad i=1,2,3 \end{aligned}\right\} \quad (2.1.-18)$$

if we start, as usual, from a steady state. This type of start up is not the one really applied for the reactor, as we shall see later on, but very convenient for analog purposes.

Now we convert the φ_j into dimensionless powers P_j by multiplying them with $1/\Lambda_j$, respectively, a relation which can be derived from definition (2.1.-7).

In order to normalize the total power

$$P(t) = \sum_{j=1}^{3} P_j(t) \qquad (2.1.-19)$$

to unity at the beginning ($P^o = 1$), we find that

$$P_j(t) = \zeta \cdot \frac{\varphi_j(t)}{\Lambda_j} \qquad j=1,2,3 , \qquad (2.1.-20)$$

where the normalization factor ζ is

$$\zeta = \frac{1}{\sum_{j=1}^{3} \frac{\varphi_1^o}{\Lambda_j}} = \frac{1}{\frac{1}{\Lambda_1} + \frac{l_2}{l_{12}^o} \cdot \frac{1}{\Lambda_2} + \frac{l_2\, l_3}{l_{12}^o\, l_{23}} \cdot \frac{1}{\Lambda_3}} \qquad (2.1.-21)$$

Of course, if some of the coefficients 1 or Λ should be time-dependent, we must use their initial values for (2.1.-18) and (2.1.-21) (see expression 2.2.-8).

The initial conditions for the $c_i(t)$ are

$$c_i^o = \frac{\beta_i}{\zeta\lambda_i} \qquad i=1,\ldots,6. \qquad (2.1.-22)$$

group i	decay constants λ_i [sec^{-1}]	effective yields β_i	$c_i^o = \frac{1}{\zeta} \cdot \frac{\beta_i}{\lambda_i}$
1	0,013	0,000214	$1,34284 \cdot 10^6$
2	0,032	0,001325	$3,37748 \cdot 10^6$
3	0,12	0,001223	$8,31489 \cdot 10^5$
4	0,32	0,002650	$6,75228 \cdot 10^5$
5	1,40	0,000815	$4,74933 \cdot 10^4$
6	3,90	0,000173	$3,62041 \cdot 10^3$
		$\Sigma\beta_i = \beta$ = 0,0064	

Table 1. Delayed neutron parameters

2.2. The input (pulsation of the system)

The system (2.1.-12) to (2.1.-15) or the equivalent formulation with φ_j and c_i is homogeneous. For $\varphi_j = 0$, it describes a steady state if the system determinant vanishes (non-pulsed stationarity condition).

In order to generate non-trivial solutions, we must disturb the system in some way. This is done by varying

some or all of the cross-sections in the operators Pr and K in time. Consequently, the coefficients k, l, and Λ become functions of time.

The new, but not surprising situation is, in contrast with the usual kinetics equations, that more or less all coefficients must be varied simultaneously [1].

At SORA, the modulation is performed by the periodic motion of the reflector piece containing no fissionable material (Σ_f = const.). Thus, the production operator Pr and the generation times Λ remain constant, whereas the other quantities will vary.

Mr. ASAOKA [2] has calculated the necessary coefficients k and l for the two extreme cases

a) moving reflector absent,

b) moving reflector present,

with a two-dimensional S_n-code in Cartesian geometry.

His values are as follows [3]:

---

1) It may be emphasized that both modifications, periodic wobbling and accidental disturbances, enter the system at the same positions.

2) See footnote p. 9.

3) The assumed distance between moving reflector and fixed fuel in the most active position is 10 mm.

coefficient x	moving reflector absent	moving reflector present	δx
$\frac{1}{k_1}$	1,040052	1,005925	0,034127
$\frac{1}{l_1}$	0,8851	0,8014	0,0837
$\frac{1}{l_2}$	0,006299	0,006116	0,000183
$\frac{1}{l_3}$	0,0002237	0,0002257	-0,0000020
$\frac{1}{l_{12}}$	0,0001412	0,0001168	0,0000244
$\frac{1}{l_{13}}$	0	0	0
$\frac{1}{l_{23}}$	0,0002593	0,0002586	0,0000007
$\frac{1}{\Lambda_1} = \frac{k_1}{l_1}$	0,851015	0,796680	0,054335
$\frac{1}{\Lambda_2}$	0,4657	0,4754	-0,0097
$\frac{1}{\Lambda_3}$	0,006872	0,009917	-0,003045

[10^8 sec^{-1}]

Table 2. Basic values for the kinetics parameters

The first observation is that, in contrast with the above statement, the $\delta(\frac{1}{\Lambda_j})$ are not zero. This effect is possibly due to a violation of Mr. SCHWALM's assumption of near-criticality (none of the two cases is a critical state), in part also to geometrical simplifications in the S_n-code.

Whereas the relative variations $\delta x/x$ are small for $\frac{1}{\Lambda_1}$ and $\frac{1}{\Lambda_2}$, the absolute value of $\frac{1}{\Lambda_3}$ is very small. The

best way to proceed is to fit the Λ_j to common values for reflector absent and present.

It seemed to be the best to determine first the parameter values pertaining to the critical state lying somewhere between the extrema. Since there is a unique reason for the parameter changes, namely the wheel motion, we assume a common variation law for all coefficients, though this is not fully proved.

If we write

$$x(t) = x_{abs} - \delta x \cdot f(t), \qquad (2.2.-1)$$

where $f(t)$ is a normalized function between 0 and 1, then

$$x^o = x_{abs} - \delta x \cdot f^o \ , \qquad (2.2.-2)$$

and f^o is the eigenvalue of the system for which it becomes steadily critical (i.e. with a certain wheel angular position).

The contributions of the delayed neutrons cancel when computing this eigenvalue. By setting $\beta = 0$ one gets the following homogeneous system from (2.1.-12) to (2.1.-15):

$$0 = \left[1 - \frac{1}{k_{1,abs}} + \delta\left(\frac{1}{k_1}\right) \cdot f^o\right] \cdot \left[\frac{1}{\Lambda_{1,abs}} - \delta\left(\frac{1}{\Lambda_1}\right) \cdot f^o\right] n_1^o$$

$$+ \left[\frac{1}{\Lambda_{2,abs}} - \delta\left(\frac{1}{\Lambda_2}\right) \cdot f^o\right] n_2^o + \left[\frac{1}{\Lambda_{3,abs}} - \delta\left(\frac{1}{\Lambda_3}\right) \cdot f^o\right] n_3^o \qquad (2.2.-3)$$

$$0 = \left[\frac{1}{l_{12,abs}} - \delta\left(\frac{1}{l_{12}}\right) \cdot f^o\right] n_1^o - \left[\frac{1}{l_{2,abs}} - \delta\left(\frac{1}{l_2}\right) \cdot f^o\right] n_2^o \qquad (2.2.-4)$$

$$0 = \left[\frac{1}{l_{23,abs}} - \delta\left(\frac{1}{l_{23}}\right) \cdot f^0\right] n_2^0 - \left[\frac{1}{l_{3,abs}} - \delta\left(\frac{1}{l_3}\right) \cdot f^0\right] n_3^0 \,. \qquad (2.2.-5)$$

By equating the system determinant to zero, f^0 comes out from a fourth degree equation to be

$$f^0 = 0{,}826933518.$$

The corresponding critical coefficient values are:

coefficient x	critical value x^0
$\frac{1}{k_1}$	1,011831240
$\frac{1}{l_1}$	0,815623
$\frac{1}{l_2}$	0,006148
$\frac{1}{l_3}$	0,0002253
$\frac{1}{l_{12}}$	0,0001210
$\frac{1}{l_{23}}$	0,0002587
$\frac{1}{\Lambda_1}$	0,806085
$\frac{1}{\Lambda_2}$	0,4737
$\frac{1}{\Lambda_3}$	0,009390

$[10^8 \text{ sec}^{-1}]$

Table 3. Critical kinetics parameter values

For consistency reasons with SCHWALM's model we attribute the determined $1/\Lambda_j^0$ values to both positions

"reflector absent" and "reflector present" so that the $\delta(1/\Lambda_j)$ become zero.

Due to the new extreme values for $1/\Lambda_1 = k_1/l_1$ and because we will not change the $1/k_1$-values, the new extreme values

$$\frac{1}{l_{1,abs}} = 0{,}838370 \cdot 10^8 \text{sec}^{-1}$$

$$\frac{1}{l_{1,pres}} = 0{,}810816 \cdot 10^8 \text{sec}^{-1}$$

follow, and $\delta(\frac{1}{l_1})$ is reduced to $0{,}027509 \cdot 10^8 \text{sec}^{-1}$. But this does not matter, since $1/l_1$ does not explicitly appear in the equations.

If we define, to compare with the usual kinetics terminology

$$k_{eff} = k_1 \left[1 + \frac{\Lambda_1}{\Lambda_2} \cdot \frac{l_2}{l_{12}} + \frac{\Lambda_1}{\Lambda_3} \cdot \frac{l_2 \, l_3}{l_{12} \, l_{23}} \right] = k_1 \cdot \frac{\Lambda_1}{\zeta} \quad , \tag{2.2.-6}$$

we can verify that k_{eff} is of course unity. We note also that, as already mentioned, k_1 is always less than k_{eff}.

Apart from the "consistency modifications", we observe that the relative variations for $1 - 1/k_1$ are about 300 %, for $1/l_{12}$ about 21 %, whereas for $1/l_2$, $1/l_3$, and $1/l_{23}$ they are as small as 3 %, 0,8 %, and 0,3 %, respectively.

In order to simplify the analog simulation (in particular to economize multipliers leading to procedure errors), we have decided to reduce also $\delta(1/l_2)$, $\delta(1/l_3)$, and $\delta(1/l_{23})$ to zero, and to take their corresponding critical values as constant parameters. In this way, the number of input places is reduced to only two, namely for $1/k_1$ and $1/l_{12}$.

Besides, it was shown by Mr. SCHWALM's digital test computations that with these 2 inputs the approximation to the result with 5 input places is already good.

The initial values for $1/k_1$ and $1/l_{12}$, built with f^o are

$$\frac{1}{k_1^o} = \frac{1}{k_{1,min}} - \delta\left(\frac{1}{k_1}\right) \cdot f^o = 1{,}011831240 \qquad (2.2.-7)$$

$$\frac{1}{l_{12}^o} = \frac{1}{l_{12,min}} - \delta\left(\frac{1}{l_{12}}\right) \cdot f^o = 0{,}0001210 \cdot 10^8 \text{sec}^{-1} . \qquad (2.2.-8)$$

They are of course equal to the critical values of table 3.

Till now, we know something about the absolute variations of the parameters, but still nothing about the shape of the universal function f(t).

For this purpose, Mr. RIEF [1] performed a number of Monte Carlo calculations for successive stationary states when turning the wheel, giving k_{eff} as function of y, the position of the moving reflector midplane against the window midplane. The geometrical window width assumed is 11,3 cm. The distance from the moving reflector to the fuel is here only 4 mm, in contrast to Mr. ASAOKA's assumption. This discrepancy is somewhat disagreeable.

Since the reflector speed is fixed at $2{,}76 \cdot 10^4$ cm/sec, 1 cm of the y-coordinate corresponds to 36,232 μsec.

The given basic table is [2]:

---

1) Personal communication.

2) These values were calculated for a reference reactor design. Better values are expected from the critical experiment.

point no. i	y_i [cm]	t'_i [sec]	k_{eff}	
0	0	0	(0,9890)	extra-polated value
1	-0,5	$-0,18116 \cdot 10^{-4}$	0,9885	
2	-1	$-0,36232 \cdot 10^{-4}$	0,9880	
3	-2	$-0,72464 \cdot 10^{-4}$	0,9862	
4	-3	$-1,08696 \cdot 10^{-4}$	0,9837	
5	-4,5	$-1,63043 \cdot 10^{-4}$	0,9798	
6	-6	$-2,17391 \cdot 10^{-4}$	0,9735	
7	-10	$-3,62319 \cdot 10^{-4}$	0,9588	
8	$-\infty$	$-\infty$	0,9400	

Table 4. The Monte Carlo calculated reactivity input $k_{eff}(t')$

The somewhat tedious conversion of these given data to the desired function f(t) is described in appendix I, in order to not interrupt too much the drift of the paper.

The result is

$$f(t) = \begin{cases} 0 & \text{if } t < -415{,}004\ \mu\text{sec} \\ f^0 + g_1 t & \text{if } -415{,}004\ \mu\text{sec} \leq t \leq +26{,}013\ \mu\text{sec} \\ p_0 + p_1 t - p_2 t^2 & \text{if } +26{,}013\ \mu\text{sec} \leq t \leq +269{,}379\ \mu\text{sec} \\ g_0 - g_1 t & \text{if } +269{,}379\ \mu\text{sec} \leq t \leq +710{,}396\ \mu\text{sec} \\ 0 & \text{if } t > +710{,}396\ \mu\text{sec} \ . \end{cases} \qquad (2.2.-9)$$

f(t) is periodic, $f(t + T) = f(t)$, where

$$T = 2 \cdot 10^{-2}\ \text{sec}$$

is the period length.

The coefficients are:

$f^o = 0,826933518$ $\quad p_o = 0,821392546$

$g_o = 1,41553902$ $\quad p_1 = 2,41856839 \cdot 10^3 \ sec^{-1}$

$g_1 = 1,992591 \cdot 10^3 sec$ $\quad p_2 = 8,18763 \cdot 10^6 \ sec^{-2}$

2.3. The approach to "pulsed" criticality

Up to this point, the overall level of the pulsed reactivity is arbitrary with respect to the "steadily critical" level $k_{eff} = 1$. It is known from the theory of differential equations with periodic coefficients that the time average of the pulsed reactivity is by no means unity but always lower, if the solution (the system output) should be periodic. Methods for calculating the mean antireactivity to make the output periodic if the input is an arbitrary periodic function are not known in general. Of course, the periodicity condition is independent of any condition for "steady criticality".

In order to solve the problem semi-empirically we introduce a "supplement" ε (to be realized by a shim rod in real performance) which we add simply to $f(t)$. This ε must be adjusted by hand by comparing the amplitudes of consecutive pulses of some output variable. The only value ε leading to the periodic solution shall be called ε_{crit}. Of course, the magnitude of ε_{crit} depends on the unessential original position of the input pulses we had chosen.

Seeing that the top value of k_{eff}, computed from Mr. ASAOKA's data, remains still below prompt criticality $1 + \beta$ (cf. fig. 1), it is obvious that the entire input must be shifted upwards to reach a periodic solution.

The observation technique to determine ε_{crit} shall be described later on. Here it is sufficient to know that the starting point f^0 lies on the increasing straight flank. Lifting the curve when this point stays where it is means that the connection point of straight part and parabola moves away from the start point and the latter remains more than before on the straight part.

Simply shifting the input curve in the ordinate direction would, however, disturb the originally consistent set of initial values for the next run so that a new reproducible start would become impossible. The adjustment of f(t) must obviously be performed in such a way that $f(0) = f^0$ will be maintained whatever the adjustment parameter ε is.

If we shift the f(t) not vertically but along its straight flank, each shifted curve intersects the f^0-level at the same point t = 0. This means that we must, when modifying the level of $1/k_{1,abs}$, at the same time shift the phase of f(t) by the suitable amount.

We introduce a shifted time variable

$$\tau = t - \frac{\varepsilon}{g_1} \qquad (2.3.-1)$$

for use on f only [1]. The representation given above for f(t) (2.2.-9), and also the limits of straight line and parabola domains may now be valid for the argument τ.

---

1) This time shift means only a modification of the origin in the DFG-unit (Diode Function Generator), and brings no complication into the simulation process. Of course, the pulse peaks will then occur at different times according to ε, later on, but the absolute time counting, referred to t = 0, is without interest.

For any time dependent coefficient x(t) of the kinetics system (2.1.-12) to (2.1.-15) holds (cf. 2.2.-2)

$$x(t) = x_{abs} - \delta x \cdot [f(\tau) + \varepsilon] \,, \qquad (2.3.-2)$$

and it can easily be seen that

$$x(0) = x_{abs} - \delta x \cdot [f(\tau)\Big|_{t=0} + \varepsilon] = x_{abs} - \delta x \cdot f^{o} \qquad (2.3.-3)$$

is independent of ε, since $f(\tau) = f^{o} + g_{1} \cdot \tau$ in the region in question.

A check calculation was performed with the aid of the MIDAS digital program [1]. It gave, always with the same initial conditions, the height of the first pulse as a function of ε. As mentioned, for $\varepsilon = 0$ the pulsed system is highly subcritical so that the first power pulse height is still much lower than the expected value for the periodic solution (about 200 times the mean = initial value), namely 6. Increasing ε up to $5{,}5 \cdot 10^{-2}$ gave $P_{max}/P = 198$. The value found subsequently on the analog computer

$$\varepsilon_{crit} = + 5{,}495 \cdot 10^{-2},$$

lay exactly on the interpolated MIDAS curve (see fig.2). This agreement is one proof that the analog program worked well.

---

1) MIDAS (Modified Integration Digital Analog Simulation) is a computer program direct outgrowth of DAS Digital Analog Simulator) for obtaining a digital solution on IBM 7090 or IBM 7094 for systems of ordinary differential equations.

Mr. d'HOOP's collaboration for MIDAS programming is here gratefully acknowledged.

2.4. The problem of large power variations

The overall characteristics of the "stationary" output pulses have been studied earlier by MISENTA (see also [4]). From there we know that the ratio between peak power (pulse top) and minimum power (between pulses) can surely be made larger than 600. The delayed neutron precursors are responsible for the background power, for they behave essentially like a constant source; their decay times are much larger than the SORA pulse period.

On the other hand, STIEVENAERT [5] observed that increasing the input reactivity span above 5β does not much improve the output characteristics.

The power value at the end of each interval between pulses is the initial condition of the power at the beginning of the successive pulse. Wishing to read with comparable accuracy both peak- and minimum-power values on a PACE 231 R computer, whose reference voltage is 100 V, two methods were investigated to overcome the difficulties arising from uncertainty in reading voltages below 1 V, namely

- the variable transform method,
- the scale factor change method.

The first method consists in considering the logarithms of the strongly varying variables. For one kinetic equation and I precursor equations, this leads to transform our linear system of $(I+1)^{th}$ order into a nonlinear system of RICCATI's type of order I. Because of the cross-products of all I+1 dependent variables, a lot of multipliers would be needed.

The new kinetic system is closed. But, in order to get the input to the system of thermal equations, one needs the power in original and not in logarithmic scale so that one comes back to the same dilemma as soon as the frame of pure kinetics is left.

In addition, for SCHWALM's system with more than one kinetic equation, the same equivalence as between a linear equation of second order and a first order RICCATI equation no longer exists, as one can show mathematically. Thus, the recourse to the scale factor change method is imperative.

This method consists in changing the scale factor automatically when crossing some fixed voltage of the most sensitive variable [1].

Since the reactivity pulse length covers only about 5,6 % of the whole SORA period T, and the behaviour of the reactor is substantially different during those 5,6 % and the remaining 94,4 %, it is convenient to examine this behaviour with two different scale factors. This on one side allows the expansion of the reactivity pulse length to cover a machine time which is enough to visualize the excursions of the most interesting variables; on the other side it keeps the machine time length of the interval between pulses within an extension such that even after 40 - 50 pulses the operational components' drift has no significant influence on the results. For the fast time scale a factor of 10^5 has been chosen and for the slow time scale a factor of

---

1) It must be pointed out that with the new generation of computers, such as, e.g. DES 1, the use of floating point arithmetic eliminates the need for amplitudes scaling.

$0,5 \cdot 10^3$. The whole system has then been split up into two systems of equations:

- S_1 with reference to the reactivity pulse,

- S_2 with reference to the interval between pulses.

Details will be given in paragraph 5.1.

3. Heat transfer

The heat transfer from fuel through the canning layer to the coolant and out of the system is described in order to take into account the thermal feedback on the one reactivity or equivalent quantities via the temperature coefficients.

Let us suppose that during the power pulse the system is thermally insulated, or that the heat diffusion from a fuel element is negligible. The mean power of the reactor is 500 kW. Since about 80 % of the total energy is generated during the pulses (results of MISENTA for a reactivity change of 5 β) the pulse energy E^0 is in the order of 1850 kW sec/m^3. The fuel temperature rise is $\Delta\bar{T}_F = E^0/\rho_F c_F \approx 0{,}8\ ^\circ C$ in each pulse. This means that the fuel temperature remains almost constant, and still more the coolant temperature because of its large time constant and the corresponding smoothing.

In other words, for the "non-disturbed" pulsed state, the thermal equations describe a quasi-trivial behaviour only. If not carefully scaled, no temperature oscillations will be recorded. The temperature coefficients are anyhow very small (some 10^{-6} $(^\circ C)^{-1}$, see paragraph 3.5) so that practically no feedback exists.

The knowledge of the applied reactivity input (magnitude of $f(t)$ times $\delta(\frac{1}{k_1})$) is probably not better than $\pm\ 10^{-3}$, whereas the amount of the temperature feedback-reactivity is only about 10^{-6}. The feedback provides thus only a practically imperceptible modification of the input reactivity pulse within a broad uncertainty band.

However, the conclusion that the thermal feedback is completely inefficacious would be not right. Whatever the

input pulse shape may be, known or unknown, periodicity is achieved with just one reactivity level, in particular near the top. The output, the power pulse height, is extremely sensitive against modifications of this level. Any adjustment only by hand would be very difficult in the simulation with its extended time scale and impossible in the quickly pulsed true performance by a shim rod. The negative temperature feedback, however small it is, provides just the automatic servo system for keeping the reactivity on the right level.

The larger is the reactor power, the larger are the periodic temperature variations, thus the stabler is the reactor. If a prototype of small power can be governed, this will be somewhat easier for a large performance [1].

Consider now perturbations from the periodic state. Only here, temperature changes could reach large amounts. In view of these excursions, the heat transfer equations shall be established with care. But before, it cannot be well decided, if all the expense for the thermal model is justified [2].

3.1. Fuel heat balance

The heat balance of any volume is the equation of FOURIER:

$$\frac{1}{a}\frac{\partial T}{\partial t} = \nabla^2 T + \frac{1}{k} W \qquad (3.1.-1)$$

where

T = temperature
a = $k/\rho c$ = thermal diffusivity
k = thermal conductivity
ρ = density

---

1) Apart from the start-up procedure.

2) In fact, it is not, as we shall see later.

c = specific heat
∇^2 = LAPLACE operator
W = heat source (per unit volume and unit time).

The coefficients a and k are supposed to be temperature-independent.

The input W is generally a function of space and time. In our case (point reactor model) it should be a function of time only.

In order to simplify the geometry we choose a simple fuel rod, the properties and behaviour of which are considered as representative for the reactor. The heat conduction in axial direction is neglected against the one in radial direction.

The only space coordinate occuring in ∇^2 is thus r. Our equation becomes (the subscript F refers to fuel):

$$\frac{1}{a_F}\frac{\partial T_F(r,t)}{\partial t} = \frac{\partial^2 T_F(r,t)}{\partial r^2} + \frac{1}{r}\frac{\partial T_F(r,t)}{\partial r} + \frac{1}{k_F}W(t). \qquad (3.1.-2)$$

The boundary conditions are:

$$\left.\frac{\partial T_F(r,t)}{\partial r}\right|_{r=0} = 0 \quad \text{(finiteness in the axis)} \qquad (3.1.-3)$$

$$-k_F \left.\frac{\partial T_F(r,t)}{\partial r}\right|_{r=R_F} = h_{FS}\left[T_F(R_F,t) - T_S(t)\right] \quad \text{(outflow)}. \qquad (3.1.-4)$$

The second condition, which gives the heat flux at the fuel surface (radius $r = R_F$), is a boundary condition of third kind. h_{FS} is a heat transfer coefficient to be

defined below, and $T_S(t)$ is the steel cladding temperature.

The specific difficulty is that both inputs $W(t)$ and $T_S(t)$ are time dependent, either in a given manner or as other variables of the complete set of differential equations.

To prepare the problem for an analog computer treatment the space derivatives must be eliminated in some way. In fact, the whole space distribution of temperature is not interesting, but only some local temperatures, say, in the axis, at the surface, and a mean temperature.

The solution has been given by Mr. PALINSKI [6]. The essential steps of his derivation are reproduced in appendix II.

Here we give directly the result:

$$\frac{d}{dt}\Delta\bar{T}_F = \frac{a_F}{k_F}\left[W^oP(t) - W_L(t)\right] \qquad (3.1.-5)$$

with

$$W_L(t) = \frac{8k_F}{(1+p)R_F^2}\left\{\left[\Delta\bar{T}_F(t) - \Delta T_S(t) + \bar{T}_F^o - T_S^o\right] - \sum_{n=1}^{\infty}\alpha_n\Gamma_n(t)\right\} \qquad (3.1.-6)$$

The symbols should be read in appendix II.

3.2. Cladding heat balance

The cladding layer is thin enough that we may consider a unique temperature $T_S(t)$. The respective heat balance has the well known form:

$$\frac{d}{dt}\Delta T_S(t) =$$

$$= \frac{a_S}{k_S}\left\{\frac{R_F^2}{R_l^2 - R_F^2} W_L(t) - \frac{2R_l}{R_l^2 \quad R_F^2} h_{SC}\left[\Delta T_S(t) - \Delta\bar{T}_C(t) + T_S^o - \bar{T}_C^o\right]\right\}. \qquad (3.2.-1)$$

$\bar{T}_C(t)$ is the (radially) averaged coolant temperature. Because W^o is a specific power per unit volume of fuel, some geometrical correction factors occur in the above equation. R_l is the inner radius of coolant ring, equal to the outer cladding radius.

The only difficulty is that h_{SC}, the "heat transfer coefficient between cladding and coolant" has no significance for liquid metal cooling if interpreted in the usual sense. This will be discussed at once.

3.3. Coolant heat balance

The coolant of SORA is eutectic NaK. The molecular heat conductivity k_C of such a coolant is very high, compared with that of water, e.g.. In fact, the heat transport by conduction is much more important than that by turbulent motion of the liquid.

Consequently, the derivation of an appropriate coolant heat balance equation calls for some rigour though we will - with a trick - obtain an equation which is formally equal to known balance equations. Details are given in appendix III.

Here we give directly the result:

$$\frac{d}{dt}\Delta\bar{T}_C(t) = \frac{a_C}{k_C}\frac{2R_i}{R_a^2 - R_i^2} h_{SC}\left[\Delta T_S(t) - \Delta\bar{T}_C(t) + T_S^o - \bar{T}_C^o\right] - \frac{2w}{L}\left[\Delta\bar{T}_C(t) + T_C^o - T_C^{in}\right] , \quad (3.3.-1)$$

with

$$h_{SC} = \frac{k_c}{R_a} \cdot 51{,}222023 . \quad (3.3.-2)$$

3.4. Compilation of parameters

W_{total}	core heat output	500 kW
N	number of active fuel rods	107
R_F	fuel radius	$7 \cdot 10^{-3}$ m
L	rod length	0,24 m
V_F	fuel volume	$3{,}9531 \cdot 10^{-3}$ m³
W^o	power density per fuel volume unit	$1{,}26482 \cdot 10^{5}$ kW/m³
a_F	fuel thermal diffusivity	$5{,}68 \cdot 10^{-6}$ m²/sec
k_F	fuel thermal conductivity	0,0138 kW/m °C
δ_G	bond thickness	$2 \cdot 10^{-3}$ m
k_G	bond thermal conductivity NaK	0,0253 kW/m °C
δ_S	cladding thickness	$3 \cdot 10^{-3}$ m
a_S	cladding thermal diffusivity (Incoloy)	$4{,}92 \cdot 10^{-6}$ m²/sec
k_S	cladding thermal conductivity (Incoloy)	0,0183 kW/m °C
h_{FS}	heat transfer coefficient fuel - cladding	42,72 kW/m² °C

p	PALINSKI's parameter	0,18459

PALINSKI's coefficients:

n	1	2	3	4	5	6	7	8	9
ρ_n	4,927	8,083	11,173	14,249	17,324	20,404	23,488	26,579	29,674
δ_n	2,814	7,574	14,472	23,536	34,791	48,257	63,952	81,887	102,074
α_n	0,479	0,447	0,408	0,366	0,324	0,286	0,251	0,220	0,194

R_i	inner coolant channel radius	$7,5 \cdot 10^{-3}$ m
$R_a \left(= \sqrt{\frac{2\sqrt{3}}{\pi} R_i}\right)$	"outer" coolant channel radius	$7,8756 \cdot 10^{-3}$ m
F_{SC}	fictive heat transfer surface between cladding and coolant (per channel)	$1,1430 \cdot 10^{-2}$ m^2
a_C	coolant thermal diffusivity	$3,43 \cdot 10^{-5}$ m^2/sec [1]
k_C	coolant thermal conductivity	0,0253 kW/m °C [1]
h_{SC}	heat transfer coefficient cladding-coolant	164,55 kW/m^2 °C
w	coolant velocity	6,00 m/sec
T_C^{in}	coolant inlet temperature	200 °C
$\bar{T}_C^{out}$	mean coolant outlet temperature	250 °C

---

[1] properties refer to 230 °C

Initial values:

$\bar{T}_F^o$	298,11 °C
T_S^o	231,61 °C
$\bar{T}_C^o$	229,10 °C

Other interesting values:

V_{core} active core volume	$5{,}004 \cdot 10^{-3}$ m³
volume fractions:	
fuel	0,79001
NaK (eutectic), total	0,13889
NaK, coolant only	0,09310
Incoloy	0,07110
power density, average	10^{+2} MW/m³ (of core volume)
average heat flux through cladding surface	41,32 W/cm²
coolant flow rate through active zone	9,5281 kg/sec

3.5. Temperature coefficients

The coefficients of SCHWALM's kinetics system are all more or less temperature dependent. Let once more x be one of these coefficients, then

$$x(t) = f[\Delta T_i(t)] \qquad (3.5.-1)$$

where, in our case, the ΔT_i are the temperature deviations

of fuel, cladding, and coolant, respectively, from their initial levels.

Let us develop $f(\Delta T_i)$ into a TAYLOR series about the origin:

$$x(\Delta T_i) = x\Big|_{\Delta T_i=0} + \sum_i \frac{\partial x}{\partial \Delta T_i}\Big|_{\Delta T_i=0} \cdot \Delta T_i + \ldots \qquad (3.5.-2)$$

$x\Big|_{\Delta T_i=0}$ is the value pertaining to the start temperature distribution.

We may stop the development after the first order terms if x depends linearly or almost linearly on the temperatures which is generally assumed for simplicity.

The first-order partial derivatives with respect to the temperatures, divided by the quantity itself, are called the temperature coefficients γ_i of the quantity in question:

$$\gamma_i = \frac{1}{x} \cdot \frac{\partial x}{\partial T_i}\Big|_{\Delta T_i=0} \cdot \qquad (3.5.-3)$$

Since the temperature propagation is rather sluggish compared to the power variations in our pulsed reactor, a marked safety or dangerous effect can only come from the most prompt temperature reactions on power, i.e. from the fuel zone.

The calculation or estimation of the numerical values of the coefficients concerns mainly neutron physics. Mr. RANDLES has kindly furnished the data asked by us [1]. Here we give only some physical considerations.

---

[1]) Personal communication.

The fuel temperature effect consists of a material expansion and the known DOPPLER effect, the uranium resonance broadening when heating up the neutrons.

The radial dilatation is allowed by the NaK bond, thus giving no modification of the average fuel density in the core. On the other hand, the axial expansion truly lengthens the rods, which leads to a negative contribution to the fuel temperature coefficient.

The DOPPLER contribution has been found to be slightly positive, about 6 times smaller than the former one.

Now, the positive DOPPLER coefficient is, without any delay, coupled with the fuel temperature. The expansion, however, comes a bit later, for it can propagate only with the velocity of sound.

Mr. RANDLES has solved the wave equation for the rod applying a temperature step at the beginning. The time required for the rod to reach again its natural length is about 120 μs for one end fixed, and about 60 μs with both ends free, hence in the order of the power pulse width, in both cases. One can estimate that for, say, 10 or 20 μs the overall fuel temperature feedback is slightly positive, after the temperature has undergone the step. Later on, the negative expansion effect becomes dominant.

Apart from the fact that the temperature rises only according to the power release, the possible positive reactivity contribution is at best $+0{,}5 \cdot 10^{-6}$ for a normal pulse. This means a modification of the applied reactivity pulse shape by a very small amount, nothing else. To reach larger contributions, larger temperature steps, and consequently larger pulse powers, would be needed. For instance, for only +1 pcm DOPPLER reactivity, the power pulse should be the 20 fold of the normal one, and this

from one pulse to the next, since meanwhile the expansion effect has destroyed the positive contribution.

Such events are by far outside the range we intend to master with an automatic control, since one would need several hundreds of pcm to call them forth, whereas 200 pcm already cause melting. Of course, in those cases, if at all possible, an emergency shut down finishes at once the process.

The conclusion is that, for normal transients, we can safely add the two fuel coefficients together so that the sum is negative.

Possibly, the bowing of the rods could provide a further negative (stabilizing) feedback. Since all temperature coefficients play the part of parameters, a further small modification of the anyhow negative fuel coefficient cannot much change the transient response so that it has been omitted.

Mr. RANDLES' temperature coefficients are all calculated for the reactivity k_{eff} of a one group model. Since the rôle of Mr. SCHWALM's fast group multiplication factor k_1 is so dominant (because of the difference $1 - \frac{1}{k_1}$), the above temperature coefficient can be applied also to k_1 with a very good approximation.

Let γ_l be one of RANDLES' temperature coefficients, defined by (3.5.-3), then

$$\frac{1}{1/k_1} \frac{\partial}{\partial T_l} \left(\frac{1}{k_1}\right) = -\gamma_l \quad . \qquad (3.5.-4)$$

All temperature coefficients to apply for $1/k_1$ have the same values as given originally, but with inverse sign.

The next question is, how is the feedback influence on the other coefficients of the kinetics equation system. As already indicated in paragraph 2.2., the relative changes of these coefficients are very small with respect to $1 - \frac{1}{k_1}$. It is therefore justified to neglect the feedback on them, and no effort has been made to calculate the corresponding temperature coefficients.

Let $F(t)$ be the feedback contribution to $1/k_1$, then

$$F(t) = \gamma_F \Delta\bar{T}_F(t) + \gamma_S \Delta T_S(t) + \gamma_C \Delta\bar{T}_C(t), \qquad (3.5.-5)$$

and expression (2.3.-2), written for $1/k_1$, is completed to be

$$\frac{1}{k_1(t)} = \frac{1}{k_{1,abs}} - \delta\left(\frac{1}{k_1}\right) \cdot \left[f(\tau) + \varepsilon \right] + F(t). \qquad (3.5.-6)$$

The numerical values of the temperature coefficients are

$$\gamma_F = -5{,}51 \cdot 10^{-6} \ (^{\circ}C)^{-1}$$
$$\gamma_S = -6{,}90 \cdot 10^{-6} \ (^{\circ}C)^{-1}$$
$$\gamma_C = -2{,}70 \cdot 10^{-6} \ (^{\circ}C)^{-1} \ ,$$

but must be applied with positive sign for our inverse quantities.

4. Control

It is obvious that reactivity corrections for SORA must be performed by means of an automatic control rod. Due to the extreme sensitivity of the system, it can be expected that the reactivity worth of this rod may be rather small. Its movement may neither be too slow so as to compensate a moderate run-away of the power nor too fast in order to avoid permanent convulsions due to noise.

4.1. The input

The first task when attacking this problem is to study from a technical point of view which quantities could serve as input for the control system. Mathematically, this is at first sight the power P(t), but, after careful examination, it revealed that there is no convenient measuring apparatus for such a rapidly varying quantity.

After all, the quantity to be maintained on a desired level is not P(t) but its time average over a period:

$$\overline{P}(t) = \frac{1}{P} \int_{t-T}^{t} P(t)dt. \qquad (4.1.-1)$$

Only deviations from $\overline{P}(t)$ should excite the control.

When integrating P(t) e.g. in a measuring chamber, formula (4.1.-1) demands to clear continuously the same time span at the lower limit as is added at the upper limit. Such a measuring device is practically not feasible.

These previous considerations call for the period

energy as control input [1]. We suppose to integrate the power from the discrete time $\hat{t}_m$ after the (m-1)th pulse till the same time after the m-th pulse, distant by the period length T. By multiplying the integral with W^o we obtain the energy

$$E_m = W^o \int_{\hat{t}_m}^{\hat{t}_m + T} P(t)dt \qquad (4.1.-2)$$

of the m-th period.

E_m is a sampled quantity. Consecutive E's are equal as long as the power P(t) is periodic but change if there is a disturbance. At each point $\hat{t}$, the counter is reset to zero in order to be ready for the integration over the next period.

Let

$$E^o = W^o T \qquad (4.1.-3)$$

be the known reference energy of a period, then the deviation

$$\delta E_m = E_m - E^o \qquad (4.1.-4)$$

is zero for periodic operation.

The figure δE_m is stored during the (m+1)th period, where it is a convenient control input. It is to be noticed that this signal inevitably enters the control only one period length later than it was generated.

It is obvious that the points $\hat{t}$ should lie somewhere

---

[1] Mr. EDER has suggested using a peak-reading voltmeter and controlling on the maximum of P(t). This alternative is possible on account of the near-proportionality of $\bar{P}$ and P_{max} (see fig.10).

between the pulses where the reactor is unsensitive in order to get time for the counter switchings. A similar recommandation holds for the simulator. In fact, we choose just the points where the time scale factor had to be changed, and when the system was anyhow stopped for about one second of machine time.

4.2. The control rod driving motor

If we deal with such fast processes as it is the case for SORA, we must carefully describe how the input signal δE_m is being transduced into a control reactivity. Introducing a factor to convert the dimension and possibly a (pure) time delay would be by far insufficient.

Several ideas about the most suitable driving mechanism had been studied which we will not all discuss in detail.

The application of a stepping motor, performing a definite number of steps (1 to 4) between consecutive periods, according to the magnitude of δE_m, had been considered. However, a motor with the desired characteristics is not feasible.

A dead-band, i.e. a strip around $\delta E_m = 0$ where the control device should remain insensitive, was long in discussion, in order to avoid rod convulsions due to noise. This question could be answered by the simulation itself: the dead-band is not necessary if the time-constants are suitably chosen (see paragraph 5.4.).

In fact, we take now the quantity δE_m, amplify it suitably by a factor $\varkappa$ and feed it to the excitation windings of a DC motor. The equation of this motor is assumed to be:

$$AB \frac{d^3K(t)}{dt^3} + B \frac{d^2K(t)}{dt^2} + \frac{dK(t)}{dt} = \varkappa \cdot \delta E_m \qquad (4.2.-1)$$

Here, K(t) means the rotor angular position so that dK(t)/dt is the rotational speed. Obviously, if the excitation is zero, the motor is at rest, but at an arbitrary position K, since K does not appear itself and its initial condition is not defined. This kind of control is called "velocity control". It is necessary in order to let return the reactor to the same power it had before it was disturbed [1].

B is the electromechanical motor time constant, namely its total inertia (of rotor + load) about the rotation axis, divided by the friction factor.

The other time constant A is that of the armature circuit, namely its selfinductivity, divided by its ohmic resistance. For a good performance, the selfinductivity is so small that A can be kept below 0,1 msec which is negligible against B.

Consequently, the first term of (4.2.-1) can be cancelled. The equation is only of first order with respect to $\dot{K}(t)$ and has no possibility of resonance frequencies.

There remain two degrees of freedom, namely the quantities $\varkappa$ and B, which can be optimized.

The desired behaviour of $\dot{K}(t)$ is a smoothed but not too slowly declining oscillation as response to any discontinuous change of the input δE_m, with as small as possible overshoots.

---

1) In the language of transfer functions: A pole in the s-origin is necessary.

In order to translate the angular position K(t) into a reactivity we choose a rotatory rod [1] where a certain sector or segment is made by reflecting material whereas the other part is empty or neutron absorbing. This is not difficult because the reactivity worth must anyhow be only small (10 pcm, as we shall see). With a proper geometry, the characteristic can be made linear, i.e. the reactivity proportional to the angular position within an angle of 180°.

The rod is, by a shaft and without gearing box, directly coupled with the rotor. In this way the load is minimized, because no weight must be moved by the motor. The common axis is vertical, and the position of the automatic rod can be somewhere in a hole of the fixed reflector.

The load (shaft + control rod) inertia should be small against the rotor inertia, as we shall see later on.

If the rod contains no fissionable material, its action on the kinetics system is just like that of the wheel reflector, i.e. mainly on $1/k_1$ and $1/l_{12}$. As already mentioned for the temperature feedback, it is not worth considering the small contribution to $1/l_{1*}$, compared with the large one from the wheel reflector. Therefore a new modification of (3.5.-6)

$$\frac{1}{k_1(t)} = \frac{1}{k_{1,abs}} - \delta\left(\frac{1}{k_1}\right)\left[f(\tau) + \varepsilon\right] + F(t) + K(t) + D(t) \qquad (4.2.-2)$$

---

1) Proposal of Mr. LARRIMORE

is sufficient.

K(t) is the above control contribution, and D(t) may be an intentional disturbance, the true input for the runs describing perturbations from the periodic state.

5. Computational aspects and results

5.1. Programming

With reference to paragraph 2.4, two systems of equations are taken into consideration:

- S_1 which describes SORA behaviour during the reactivity pulse length,
- S_2 which describes SORA behaviour from each reactivity pulse end to the beginning of the successive pulse.

S_1 end conditions are S_2 initial ones and vice versa for successive pulses.

Furthermore, S_1 includes three subsystems or "groups":

- the first one (00) refers to lower values of all variables exceeding sometimes a certain given reference level,
- the second one (01) refers to upper values of all variables exceeding sometimes a certain given reference level,
- the third one (02) refers to other variables.

S_2 is only one "group" (03).

Hence, it appears that the treatment of SORA equations on an analog computer can only be performed if one disposes of both analog and digital computing facilities. Actually, this is a typical case of analog computation under digital control [8].

At CETIS-CANA electronic laboratory, a SIOUX [1] unit has been constructed [9]; through pulse instructions it allows the following "modes" of operation for integrators:

- Initial Conditions (IC)
- Operate (OP)
- Hold (H) .

An integrator, controlled through SIOUX [2], can only be put in IC, for instance, when the relative pulse gets to its IC coil; hence, the definition of "group" becomes evident in as much as it defines components operating in the same sequential "mode".

CETIS has contributed the report [10] in the definition of a special language for drawing computing block diagrams; according to the above concepts, they will from now on include both analog and numerical components [3].

Fig. 3 a) and b) represent:

- a) the "group" or analog element of the hybrid block diagram; it is a vector. Through IC, OP, H instructions can be given to the "group";
- b) the "command program" or numerical element of the hybrid block diagram, which possibly includes

---

1) Sequential Iterative Operation Unit X groups. Version 2 of SIOUX has been set up so that it could easily be inserted on a PACE 231R console and patched with normal patch-cords.

2) SIOUX is suitable to control problems such as: a) automatic scale factor change, b) boundary conditions, c) iterative processes in general.

3) In the writers' opinion this is the best definition of the notion of "hybrid".

manual commands (MAC).

In Fig. 3 a) and b), the instructions are represented with dotted lines, starting from the command and getting to IC, OP, H. Such instructions can be delayed through delay units (CD).

The sequence of SORA "modes" of operation is shown in fig. 4. The first period starts manually by putting groups 00 and 02 in OP, while groups 01 and 03 stay in IC; 01 tracks the variables of 00. A comparator of group 00 marks the crossing of a certain reference level, puts the 00 and 02 in H, and, after some delay for the time constants of the R-C initial condition network, 01 and 02 in OP; 03 remains in IC etc., according to fig.4. After the end of the first period the process starts again automatically through CD4.

Fig. 5 gives the hybrid block diagram which refers to the sequence in fig. 4.

APACHE [11] [1] and SATANAS [12] [1] have been used for programming the classical part of the dynamic system. All variables, excepted fluxes and powers, have been treated as perturbations and recorded, excepted for a limited number of cases, on 8-channel recorders, because of the unusual length of the runs.

In addition, the particular feature of the SORA control loop (definite integrals to be stored) requested special external circuits [2]; for these, manual programming techniques have been adopted. Such circuits were prepared in close collaboration with CETIS-CANA electronic laboratory.

---

1) Analog Programming And CHEcking
Semi AuTomatic ANAlog Setting

2) for whose set-up Mr. Van WAUWE's valuable collaboration is here gratefully acknowledged.

5.2. The periodic pulse characteristics

As already mentioned in section 2, we must first reach the periodic, non-perturbed state as the initial state for the disturbances. Though the characteristics of the periodic pulses were approximately known by digital computations of Mr. MISENTA and of Mr. SCHWALM, this part of the work consumed more time than the subsequent disturbance runs.

The following variables have been recorded [1]:

- the input $f(t)$
- the output $P(t)$
- the output $P^{(2)}(t)$ (upper part of $P(t)$ only)
- the integrated power $\int P(t)dt$ (definite integrals over one period)
- the precursor density $c_3(t) - c_3^0$
- the fuel temperature $\Delta\bar{T}_F(t)$.

All dependent variables become periodic with period T, as repeatedly said, for one and only one value of ε ($= \varepsilon_{crit}$), which we can therefore call the pulsed criticality parameter. It is independent of any criticality parameter (e.g. k_∞) for steady state.

When checking the periodicity of all recorded variables, it turned out that the most sensitive reading was that of $c_3(t) - c_3^0$ because the precursor density changes from their initial values are anyhow small and can be represented by the whole available ordinate.

---

1) The recording precision has not been embellished. Slight discrepancies must be seen in this light.

The critical value found in this manner was

$$\varepsilon_{crit} = +5{,}495 \cdot 10^{-2} \ .$$

The input, shifted by just this value, is also represented in fig. 1 (solid curve).

The critical values for periodicity pertaining to ε_{crit} are:

$$\left(\frac{1}{k_{1,max}}\right)_{crit} = \frac{1}{k_{1,min}} - \delta\left(\frac{1}{k_1}\right) \cdot \left[1 + \varepsilon_{crit}\right] = 1{,}004050$$

$$\left(k_{1,max}\right)_{crit} = 0{,}995966.$$

Note that the maximum k_1 is below unity, as it must be, because of the contribution from the other energy groups.

With $\varepsilon = 0$, the not corrected maximum was $k_{1,max} = 0{,}994110$ so that the applied ε-shift corresponds to a $\Delta k_1 = +0{,}001856$.

The minimum values are:

$$\left(\frac{1}{k_{1,min}}\right)_{crit} = \frac{1}{k_{1,min}} - \delta\left(\frac{1}{k_1}\right) \cdot \left[0 + \varepsilon_{crit}\right] = 1{,}038177$$

$$\left(k_{1,min}\right)_{crit} = 0{,}963227.$$

For the critical extrema of l_{12}, we got

$$\left(\frac{1}{l_{12,max}}\right)_{crit} = \frac{1}{l_{12,min}} - \delta\left(\frac{1}{l_{12}}\right) \cdot \left[1 + \varepsilon_{crit}\right] = 1{,}155 \cdot 10^{6}\ \text{sec}^{-1}$$

$$\left(\frac{1}{l_{12,min}}\right)_{crit} = \frac{1}{l_{12,min}} - \delta\left(\frac{1}{l_{12}}\right) \cdot \left[0 + \varepsilon_{crit}\right] = 1{,}399 \cdot 10^4 \, sec^{-1}.$$

For k_{eff}, defined by (2.2.-6), we found

$$\left(k_{eff,max}\right)_{crit} = 1{,}007212$$

$$\left(k_{eff,min}\right)_{crit} = 0{,}976401 \ .$$

The overshoot over $1 + \beta = 1{,}0064$ (prompt criticality) is thus 0,000812 or 81,2 pcm.

The Δk_{eff} between maximum and minimum is 0,030811 or about 4,8 β.

All these values can be seen on fig. 1, where the solid curve is the input pertaining to pulsed criticality.

The period averaged value of k_{eff} is as low as 0,977118, thus not much different from the background level.

The resulting output P(t), as it came out with scale factor changes, is represented in fig.6. In fig.7 the same output is plotted in a logarithmic scale.

These graphs confirmed Mr. SCHWALM's previous calculation to such an extent that it was not necessary to record also the group powers $P_j(t)$, or group fluxes $n_j(t)$. Their recording would have been somewhat expensive due to the scale factor changes also for these variables.

From the figures one reads the following characteristics:

- the power maximum is 194 times as high as the mean power,
- the power pulse width at half its height is 68 μsec,
- the pulse decrease is steeper than its increase,
- the power maximum occurs 55 μsec after the reactivity maximum, just when the reactivity falls again below $1 + \beta$,
- 80 % of the period energy is released in the pulse itself.

When looking at fig. 8, we must consider that the first power pulse is always incomplete, because the start of the run is on the upper part of the increasing straight flank of the reactivity pulse. The corresponding peak values of the variables may thus not be considered when checking the periodicity of the solution, nor may the power integral be taken for the control input.

Nevertheless, it turned out that the set of initial values lies so well on the desired particular integral that practically no transients could be observed. The second pulse is already representative.

5.3. Reactivity step without control

A step of D(t), corresponding to $\Delta(\frac{1}{k_1}) = -4{,}3$ pcm or $\Delta k_{eff} = +4{,}0$ pcm was applied at the beginning of a reactivity pulse (strictly speaking, where the P scale factor is being reset, because there an artificial break is introduced), when every control loop was still switched off.

The resulting power divergence is plotted on fig. 9.

One observes the known "prompt jump" immediately after the disturbance and then a slower increase due to the asymptotic reactor period when comparing consucutive maxima.

The first steep increase is unavoidable because it takes place mainly in the first pulse itself. It is quite clear that there is no control which would be able to counteract such a process, at least since its information must first be got from the whole preceding period.

But the "plateau" after the prompt jump suggests that one would win some time, and the control time constant should not in any case be extremely small. It will be shown that this reasoning is only partly valid.

5.4. Reactivity steps with low control time constant

The control system equation adopted is (4.2.-1) where the circuit time constant A is zero.

For the motor time constant B, which is explained in paragraph 4.2., we took first B = 33 ms [1]. With that B a number of runs has been recorded.

First we consider a reactivity step of Δk_{eff} = +16 pcm at the beginning of a pulse (always when P(t) is switched from $P^{(1)}(t)$ to $P^{(2)}(t)$). The step height is certainly exaggerated with respect to true events and, moreover, the reactivity rate also can never be infinitely large. Nevertheless, this worst case gives a good insight into the reactor behaviour with control.

The amplification $\varkappa$ was optimized so as to get minimum duration of transients. With too large a $\varkappa$, the system

---

1) The feasibility of this figure is discussed in paragraph 5.8.

tends to oscillate with weak damping. If $\varkappa$ is too small the restoring force is too small and the power will not return to the desired value in a reasonable time.

Fig. 10 [1] shows the behaviour with the already optimized $\varkappa$. For this optimum gain, we found

$$\varkappa_{opt} = +2{,}75 \cdot 10^{-6} \frac{m^3}{kWsec^2} \quad [2].$$

It must be pointed out that this value pertains to B = 33 ms only. Furthermore, $\varkappa_{opt}$ must be inversely proportional to the specific power W^o which is assumed. This can be seen as follows:

We have

$$E_m = W^o \int_{\hat{t}_m}^{\hat{t}_m + T} P(t)dt \qquad (5.3.-1)$$

and

$$E^o = W^o T \,, \qquad (5.3.-2)$$

thus

$$\delta E_m = W^o \left[\int_{\hat{t}_m}^{\hat{t}_m + T} P(t)dt - T \right] . \qquad (5.3.-3)$$

---

1) For reproduction reasons the curves cannot be plotted here in their original size as recorded. The pulses' shape being already given in other figures, we schematize P_m and E_m by simple lines with proper amplitude. The control output K(t) has first been modified to be understood in terms of k_{eff} (instead of $1/k_1$) before having been plotted. The periodic fuel temperatur oscillations have been subtracted for the represented curve $\Delta T_F(t)$ so that only a line connecting equivalent points of the periods is shown.

2) The first estimated value was $+10^{-6}$ $m^3/kWsec^2$.

Since the control input proper is the bracket square, we can only optimize $\varkappa \cdot W^{o}$. Thus, the larger is W^{o}, the smaller should be $\varkappa_{opt}$, and vice versa, for having the same optimum transient behaviour. This is obvious from the dimension of $\varkappa$.

With the mentioned $\varkappa_{opt}$, the transient period of the control device is as low as about 40 periods [1], or roughly 0,8 sec after the very exaggerated disturbance. At the end, the antireactivity introduced by the automatic fine control rod compensates approximately the applied perturbation step.

From fig. 10, we see further that about three oscillations occur before the system comes practically to rest. Consequently, the monotonic approach to the final control rod position is superposed by a wave-like behaviour. The maximum rod velocity (see the dotted tangent) is something like 88 pcm/sec during 0,05 sec.

Nevertheless, this high value was not adopted for the control specifications. A rate of 20 pcm/sec should be sufficient, because the applied +16 pcm-step greatly exceeds the specified reactivity worth ± 5 pcm of the fast control rod. Step perturbations of more than 4 or 5 pcm must therefore provoke an emergency shut down. Indeed, non-accidental reactivity fluctuations of this order are very unlikely. On the other hand, a controllable perturbation cannot occur as a step but with a maximum rate of +4 pcm/period, say. As a whole, every event to be considered is at best 4 or 5 times less severe than the examined case. It is not desirable to increase the rod worth over 10 pcm for a good sensitivity against small fluctua-

---

1) It should be mentioned that 40 periods take more than 1 hour of machine time.

tions (10 pcm $\hat{=}$ 180° angle), nor do we like to increase the insertion rate too much for safety. Thus, the 20 pcm/sec was chosen.

After 40 periods, the fuel temperature has not yet reached its starting level (see fig. 10), but contributes still about -1,8 pcm to the reactivity balance. The heat discharge being slow, the process can obviously not have finished before the corresponding energy is carried away by the coolant. This indicates that a certain remainder of the transient cannot be accelerated by control means since it comes from the temperature feedback. But fortunately this contribution is in the order of only one tenth of the artificially steered reactivity so that it can be neglected.

Considering different reactivity step heights (results not worthwhile to be represented graphically in detail), one observes that the absolute maximum always occurs in the second pulse after perturbation. The first and second pulse heights for various steps are (fair reading precision):

Δk_{eff} =	"steady" pulse	1st pulse	2nd pulse
+16 pcm	194	262	278
+ 8 pcm	194	250	262
+ 4 pcm	194	225	234

The first pulse is not yet influenced by control whereas the second is. But also the first pulse overshoot is not well proportional to the applied reactivity step, but tends to diminish relatively for larger disturbances. This shows that not even during the prompt jump the "transfer function" for the mean power is approximately

constant, nor exists a unique sensitivity. The latter falls from about 4 %/pcm for a 4 pcm step over 3,6 %/pcm for an 8 pcm step to about 2,4 %/pcm for the 16 pcm step (always up to the first pulse only). A linearized theory is thus not applicable, not even for small perturbations of a few pcm.

In another run, a 16 pcm reactivity step was applied not during the increasing pulse flank but somewhere between pulses. As expected - the reactor is quite insensitive between pulses - no difference could be observed compared to the former case; pulse 1 is always the one following the disturbance, whereever that was applied.

5.5. Controlled reactor behaviour with reactivity noise

The response to noise is an interesting problem because such noise can possibly not well be diminished or avoided.

Due to the fact that the reactor is only pointwise sensitive, it suffices to consider the discrete reactivity levels due to the noise, which exists in these points.

For the noise, the following assumptions have been made:

- the probability of deviations from zero level is GAUSSian-distributed,
- the variance (e.g. 99 % of the events lie between $\pm$ 2 pcm) is a variable parameter.

In order to generate a sequence of reactivity values obeying this law, several sequences of equally distributed 2-figure random numbers r_i have been taken from a statistical table. If 99 % of the events shall be included be-

tween $\pm a_0$ pcm, the abscissa a_0 of the GAUSS curve is $\pm 2{,}58$. Now we subdivide the abscissa into 5 parts:

$$\begin{aligned} u &\leqslant -0{,}75\ a_0 \\ -0{,}75\ a_0 &\leqslant u \leqslant -0{,}25\ a_0 \\ -0{,}25\ a_0 &< u < +0{,}25\ a_0 \\ +0{,}25\ a_0 &\leqslant u \leqslant +0{,}75\ a_0 \\ +0{,}75\ a_0 &\leqslant u \end{aligned}$$

and read the corresponding GAUSS ordinates of the limit points.

We check the random numbers r_ι according to whether they fall into one or another of the just found ranges of the total interval 00 to 99 and attribute them the discrete values

$$\begin{aligned} +x \quad &\text{for} \quad 99 \geqslant r_\iota \geqslant 97 \\ +\tfrac{x}{2} \quad &\text{for} \quad 96 \geqslant r_\iota \geqslant 85 \\ 0 \quad &\text{for} \quad 84 \geqslant r_\iota \geqslant 15 \\ -\tfrac{x}{2} \quad &\text{for} \quad 14 \geqslant r_\iota \geqslant 03 \\ \text{and} \quad -x \quad &\text{for} \quad 02 \geqslant r_\iota \geqslant 00, \end{aligned}$$

where x can mean 1, 2, or more pcm, at choice.

Some random sequences of reactivity levels 0, $\pm \frac{x}{2}$, $\pm$ x pcm have been fabricated in this manner and give a recipe how to vary D(t) artificially at the beginning of each pulse. Of course, 0 is the most frequent event which means to do nothing. For the other values, one keeps enough time to make the prescribed steps by hand, for one has a switching break when the SIOUX unit changes the mode (in order to eliminate switching time errors).

x was increased up to 2 pcm. No interesting effect could be observed. The power peaks obviously fluctuated a

bit but showed in no case any self-amplifying effect. This was expected because the system is stable and a sequence of reactivity steps can never be worse than when one applies all steps at once. So the former experiment with the single 16 pcm step was by far harder for the system. It is proved that the chosen control system can also master reactivity noise in the range of ±2 pcm, even more, without oscillation danger. A dead-band about the zero level, where the control is insensitive, was not simulated, but proved to be not necessary.

5.6. Shut down behaviour

Shut down simulation means the introduction of negative reactivity ramps with appropriate slope.

It is clear that, with sufficiently steep ramps, the power pulses must rapidly break down. The question is what the temperatures do in order to see if the thermal stresses will be tolerable.

The calculation of the stresses themselves falling beyond the scope of this investigation, we simply discuss the respective temperature transients.

The result is that, for -60 pcm/period, the power peaks fall below 1 % of their steady height in the third pulse after the ramp beginning, whereas for -120 pcm/period (both slopes are design reference values), the 1 % is passed under already in the second pulse.

Such a power shutdown is practically instantaneous as concerns the heat transfer from the fuel so that the temperature decrease is determined by the coolant heat transport only, assuming a step of the source from full power to zero. It does really not matter whether we apply

-60 or -120 pcm/period.

During the first four periods the fuel temperature falls by 2 °C, that of the canning by 0,2 °C, and that of the coolant by 0,2 °C also, for the -60 pcm/period ramp. For the steeper ramp the fuel temperature falls by 3 °C, whereas the other temperatures behave as above.

The subsequent temperature behaviour has not been recorded, because it can be computed simply by hand (analytic solution of FOURIER's equation after negative source step).

This experiment shows that SORA is particularly easy to scram due to its extreme sensitivity. A small amount of antireactivity (e.g. -400 pcm, where the wheel remains at constant speed) suffices to let break down the power completely. It is thus allowed to introduce the large remainder of the shutdown reactivity with considerable leisure. This will facilitate the design of the safety devices appreciably.

5.7. Reactivity steps with larger control time constants

It is quite obvious that one must investigate whether a motor time constant of B = 33 ms can really be achieved. Before answering this question in the next paragraph, we will study what happens if B is considerably larger.

First, runs have been performed with B = 100 ms. The control amplification $\varkappa$ must once more be optimized. It turned out that, with respect to the former runs, $\varkappa$ now was by far too large (as expected).

With $\varkappa = +3 \cdot 10^{-6} \frac{m^3}{kWsec^2}$ (comparable to the old value), too large oscillations of P(t) were recorded. The step

Δk_{eff} = +16 pcm lead to the known power peak overshoot for the first two pulses, but then a rather complete breakdown of the power (only about 1 % of the "stationary" peak power in the sixth pulse after perturbation) appears. The run was stopped there.

Consequently the control counterforces have been weakened by diminishing $\varkappa$ successively over $2 \cdot 10^{-6}$; 10^{-6}; $0{,}5 \cdot 10^{-6}$; $0{,}25 \cdot 10^{-6}$ down to $0{,}125 \cdot 10^{-6}$ $\frac{m^3}{kWsec^2}$.

The result was quite unsatisfactory. With medium $\varkappa$-values, the very small amplitudes could not be avoided, but occurred now later, say in the 12th pulse after perturbation, for $\varkappa = 10^{-6}$ $\frac{m^3}{kWsec^2}$. For still smaller amplifications $\varkappa$, the minimum pulse locus migrates away. With $\varkappa = 0{,}125 \cdot 10^{-6}$ $\frac{m^3}{kWsec^2}$, the behaviour is such that the control can just hinder the power divergence (as would occur without control), but shows also no reasonable restoring force. Once the high power peak is reached (at the second pulse), the peak level remains practically constant up to the 40th pulse where the run had to be stopped. Of course, the efficiency of the control had been reduced to nearly zero. It is hopeless to achieve a reasonable solution in this way.

Nevertheless, the reactor behaviour is easy to understand. The time constant B = 33 ms was still in the order of the period length (20 ms), whereas the new one is not. With B = 100 ms the control is a priori unable to follow the evolution of the power in the reactor-own time scale, it comes always too late.

For curiosity, similar runs have been performed with B = 200 ms. The phenomena were only accentuated without possibility of a solution, of course.

A rather obvious idea would be to improve the transient behaviour by introducing a phase-lead through an additional differential control term. It is to be noted that this method is not feasible for SORA. The control input δE_m is a discontinuous quantity, whose derivative is normally zero and makes only occasional delta jumps. The derivative is therefore unsuitable for a supplementary control input.

On the other hand, due to the DC-motor equation, K(t) is indeed continuous and has a reasonable derivative, but is the output of the control. It is already the rotor angular position itself and not any electrical quantity to which one could add some other term.

In simple words, it is in general possible to shift the phase of an input quantity, but never that of the desired output. From a logical point of view, an output phase-lead would need some knowledge of the future, what is of course meaningless.

5.8. Feasibility of small control time constants

This paragraph is not a result of the analog simulation but a necessary additional consideration [1].

In order to check if a time constant B in the order of 33 ms is feasible we consider two DC-motors:

---

1) This work has been performed by Mr. MARCILLAT of the ISPRA center.

type	power [1] [Watt]	rotor inertia [1] [g cm^2]	motor time constant [1] [ms]
SERVALCO TM 910	50	4500	20
DIEHL	10	17	11

The SERVALCO motor has a printed rotor (without insulation material) and requires relatively strong armature currents.

Since the force for moving the rotatory fast control rod is obviously very small, the weak DIEHL motor seems to be sufficient on first sight.

However, when calculating the inertia of the shaft between motor and active part of the control rod, one finds as much as 335 g cm^2, if it is made by aluminium, is 2 m long, and has a diameter of 1,5 cm. The inertia of an equally sized iron shaft is even 2,9 times as high. Thus, with the aluminium shaft, the total time constant of the SERVALCO system rises to

$$20 \cdot \frac{4500 + 335}{4500} = 21{,}5 \text{ ms}$$

and with the iron shaft to

$$20 \cdot \frac{4500 + 972}{4500} = 24{,}3 \text{ ms},$$

whereas the corresponding values for the DIEHL system are

---

[1]) from maker's specifications

$$\text{(aluminium)}\quad 11 \cdot \frac{17 + 335}{17} = 228 \text{ ms}$$

$$\text{(iron)}\quad 11 \cdot \frac{17 + 972}{17} = 640 \text{ ms.}$$

The latter values are by far inacceptable for SORA. A gear box with speed reduction ratios of x : 1 would reduce the system inertia to the $(1/x^2)$-fold of its former value (e.g. x = 5).

The precision of static position of the last toothed wheel may be 30'. However, the angular position itself of the control rod is more or less irrelevant since we need a velocity control system only. This imprecision is thus not dangerous, but unpredictable vibrations and twists of the rod due to the reactivity noise are to be feared. With the incessant forth and back movement of the rod, a considerable wearing of the gearings is unavoidable. This soon leads to a non-negligible play with resonance danger for certain plays.

The conclusion is that we must avoid every transmission gearing between motor and rod. Consequently, the rotor inertia must be much higher than that of the load, and the motor becomes apparently rather strong with respect to the small mass to move.

Moreover, with the strong SERVALCO motor, one is rather independent from engineering modifications of the shaft, whereas this is not the case with the weak DIEHL motor (see total time constants above).

Another advantage of the SERVALCO motor is the lack of insulation material. It could thus be placed, if

desired, into the radiation field, and consequently the shaft length be reduced.

5.9. Operation at low power

A regular operation at low power means that

- the control set point is well adjusted to this power,
- the coolant flow rate corresponds to the power.

This could be the case for instance during the starting period of the reactor.

For such a power the core temperature distribution is different. The modified ratios of the mean material temperatures enter the equations by the initial conditions but pertain also to an equilibrium.

The feedback on the reactivity is based only on the deviation from the initial values, and these are roughly proportional to the power. The extreme case we can consider is that the temperature feedback vanishes completely.

We saw already that this feedback is almost negligible also for full power. Nevertheless, we have removed the feedback F(t) completely for one run. No significant difference in pulse evolution after a reactivity step could be observed against the former case.

The dynamic behaviour for low and high power is thus practically equal. The different optimization of the control gain $\varkappa$ must, however, be regarded (see paragraph 5.3.). For low power, the chance of relative power peak fluctuations due to neutronic noise in the background between pulses is increased and must be overcome by a stronger control (larger $\varkappa$).

6. Conclusions

We compile the principal results from the dynamic studies.

First of all, the SORA reactor is controllable, if the control input is the difference between the energy of the preceding period and the reference period energy. A peak power control input is also allowed. The decision may be made from pure instrumentation point of view.

A DC-motor, working without gear box through a single shaft on a rotatory fast control rod, is the most promising solution for a fast acting regulating rod.

The rotor inertia should be much higher than the shaft inertia about their common axis.

The total (rotor + load) time constant should in no case be larger than 50 ms (better 20 - 30 ms).

The maximum reactivity insertion rate of the fast automatic control rod should be 20 pcm/sec (= 60 rpm, if 10 pcm $\hat{=}$ 180° angle).

The decline period of the optimized control is about 0,8 second at maximum.

A reactivity noise with amplitudes up to $\pm$ 2 pcm (99 % of cases) gives no trouble. Even somewhat higher fluctuations are probably allowed. A dead-band is not necessary.

The power shutdown in emergency cases can be considered as being instantaneous for heat transfer purposes. A fast insertion of +400 pcm with 60 pcm/period rate is sufficient. The remainder of the antireactivity (compensation of the moving reflector block) can be introduced slowly.

The wheel may never be stopped or brusquely braked during scram, but only afterwards.

The low power transient behaviour resembles the one at full power if the control amplification is properly adjusted.

For perturbations of inlet temperature or of flow rate, the controlled reactor behaves like a constant heat source, because the reactivity decline period is much shorter than the accumulation time of feedback-reactivities due to such perturbations. For long time investigations, the model of the controlled reactor is thus simplified to the relation

$$T_A = T_E + \text{const.}$$

(outlet temperature = inlet temperature + constant source term).

They can therefore be performed with known classical means without treating the core dynamics again in detail.

Acknowledgement

The authors wish to thank Mr. J. LARRIMORE, leader of the SORA Project, for valuable advices and criticisms.

APPENDIX I

Fitting of the input pulse shape

When considering table 4 (p. 23), the first remark is that the k_{eff}-span is perceptibly larger than that of Mr. ASAOKA. However, for consistency reasons with the other parameters, we are obliged to keep those values so that we must compress the above span. We shall anyhow utilize only the shape for our function f(t), but we must emphasize that, due to the broadened pulse, all further results will be based on ASAOKA's values and not on RIEF's ones. A decision between these data cannot be made here. Whereas the outcoming output pulse characteristics will depend on them, the essential results on the control performance will fortunately be rather unaffected.

The precision of the k_{eff}-values may be in the order of $\pm 10^{-3}$, a statement which is, however, very problematic.

We assume that the shape of $1/k_{eff}(t')$ represents the common input function shape f(t). The difference of the extreme values of $1/k_{eff}$ is $\delta(1/k_{eff}) = 0{,}052707$. This span is expanded to unity, and the value for $t' = -\infty$ set equal to zero, giving the "Monte Carlo input function $\tilde{f}(t')$" as follows:

point no.	t' [sec]	$\tilde{f}(t')$	
0	0	1	extrapolated value only
1	$-0,18116 \cdot 10^{-4}$	0,99030	
2	$-0,36232 \cdot 10^{-4}$	0,98058	
3	$-0,72464 \cdot 10^{-4}$	0,94553	
4	$-1,08696 \cdot 10^{-4}$	0,89664	
5	$-1,63043 \cdot 10^{-4}$	0,81987	
6	$-2,17391 \cdot 10^{-4}$	0,69456	
7	$-3,62319 \cdot 10^{-4}$	0,39576	
8	$-\infty$	0	

Table 5: The normalized Monte Carlo input function

For a reason which will at once become clear, it is desirable to represent this curve by an analytic expression. Since it must be symmetric about $t' = 0$, its TAYLOR expansion has no odd terms. If we neglect terms from the fourth order, the curve has obviously a parabolic vertex. A visual inspection of the given curve $1/k_{eff}(t')$, surrounded by the mentioned imprecision band, shows, however, that a parabolic continuation till $\tilde{f} = 0$ would be very bad. A straight flank continuation is by far better. Also this curve does still not represent the tails towards $t' \rightarrow \pm \infty$. But since the system is strongly subcritical in these regions and the corresponding reactivity level does not influence the output characteristics it is well justified to produce the straight lines down to $\tilde{f} = 0$, i.e. neglect the tails.

Let be

$$\left.\begin{aligned} g(t') &= a + bt' \quad \text{the straight part} \\ \tilde{p}(t') &= c - dt'^2 \quad \text{the parabolic part} \end{aligned}\right\}. \qquad \text{(AI-1)}$$

The absolute term c is not necessarily unity because the top value of $\tilde{f}(t')$ is only an extrapolated value which should not be considered.

A look on a graph of $\tilde{f}(t')$ shows that the parabola should meet as well as possible the points 1, 2, 3, and 4 of table 5, whereas the other ones pertain to the straight part.

A least square demand

$$\sum_{i=1}^{4} \left[\tilde{p}(t_i') - \tilde{f}_i \right]^2 = \text{minimum as function of c and d} \qquad \text{(AI-2)}$$

leads to

$$\tilde{p}(t') = 0{,}991212 - 8{,}11568 \cdot 10^6 \, t'^2 \quad (t' \text{ in seconds}). \qquad \text{(AI-3)}$$

This parabola does not yet hit unity for $t' = 0$. Dividing through by 0,991212 gives the new parabola:

$$p(t') = 1 - 8{,}18763 \cdot 10^6 \, t'^2 \quad (t' \text{ in seconds}). \qquad \text{(AI-4)}$$

Of course, $\tilde{f}(t')$ should be divided by the same figure to see which values are to be approximated, excepted the one for $t' = 0$ which we keep at unity, leading to a "corrected" $\tilde{f}(t')$. Then, a back-computation shows that a better extrapolation value for $k_{eff}(0)$ would have been 0,988547 instead of 0,9890, at least if one assumes that the shape in its vicinity is a pure parabola.

If we demand the connection conditions

$$p(t'_a) = g(t'_a) \qquad \text{and} \qquad \left.\frac{dp}{dt'}\right|_{t'_a} = \left.\frac{dg}{dt'}\right|_{t'_a}, \qquad \text{(AI-5)}$$

for an abscissa t'_a to determine, and that the straight line goes through the (corrected) point 7 of table 5, we have just three equations for the three unknowns a, b, and t'_a.

One finds for the increasing flank

$$g(t') = 1{,}12123221 + 1{,}992591 \cdot 10^{3}\ t' \quad [1] \qquad (t' \text{ in seconds}), \qquad \text{(AI-6)}$$

and at the connection point $t'_a = -1{,}21683 \cdot 10^{-4}$ sec the common value of $g(t')$ and $p(t')$ is 0,87877.

Fig. 1 shows that the analytical approximation of Mr. RIEF's normalized data is perfect [2].

As already mentioned at the initial conditions (2.1.-18), we assume that the reactor is steadily critical before beginning to wobble its reactivity. Thus, the first pulse must start from the height f^0 and is "incomplete" compared with the following pulses. Any other type of starting procedure would be irreproducible, because the steps "operate" and "pulsation beginning" do not coincide in the analog computer and the variables would run away in an uncontrollable manner if not all derivatives first vanish.

---

1) One calculates always with an exaggerated number of decimals in order to avoid rounding errors and inconsistencies in the analog machine setting, where initial errors would integrate with time.

2) The absolute level of the curve or, respectively, the shift from the dotted curve to the solid one will be discussed later on.

We shift the somewhat arbitrary time base start to the value $t_o' = 1{,}47696 \cdot 10^{-4}$ sec, pertaining to f^o, by introducing the new time variable

$$t = t' - t_o' \qquad \text{(AI-7)}$$

The beginning of a run is now at $t = 0$ where t is the independent variable of all system equations.

Having done this, we find the representation of $f(t)$ given at the end of paragraph 2.2.

APPENDIX II

Solution of FOURIER's equation with time dependent heat source and boundary temperature

Following PALINSKI [6], equation (3.1.-2) is LAPLACE-transformed with respect to time. The result is an ordinary differential equation with respect to r, containing the complex quantity s as a parameter. This equation can easily be solved, taking into account the transformed boundary conditions (3.1.-3) and (3.1.-4).

Now the solution is averaged over r (integral mean value), giving the mean transformed temperature $\tilde{\bar{T}}_F(s)$ as a function of s only. Due to the permutability of the linear processes of LAPLACE transformation and integral averaging, this function is just the LAPLACE transform $\tilde{\bar{T}}_F(s)$ of the mean temperature $\bar{T}_F(t)$ of the original domain, but with algebraic dependency of both inputs W(t) and $T_S(t)$. Since these two quantities are not specified, $\tilde{\bar{T}}_F(s)$ cannot be transformed back in general terms.

For this reason, the solution in the complex domain is put into the form (the snake means always the LAPLACE-transformed variables):

$$s\tilde{\bar{T}}_F(s) = \frac{a_F}{k_F}\tilde{W}(s) - \varphi(s)\left[\tilde{\bar{T}}_F(s) - T_S(s)\right], \qquad \text{(AII-1)}$$

where $\varphi(s)$ is a transfer function replacing the simple time-independent heat transfer coefficient h_{FS}. $\varphi(s)$ itself should be independent of both W(t) and $T_S(t)$.

The universal function $\varphi(s)$ can thus be transformed back, giving a function

$$G(t) = \mathcal{L}^{-1} \left\{ \varphi(s) \right\} \qquad \text{(AII-2)}$$

which is called the GREEN's function of the problem. Equation (AII-1) becomes in the original domain

$$\frac{d\bar{T}_F(t)}{dt} = \frac{a_F}{k_F} W(t) - G(t) * \left[\bar{T}_F(t) - T_S(t) \right] . \qquad \text{(AII-3)}$$

This is just the desired ordinary differential equation for the mean fuel temperature. $G(t)$ replaces the usually applied heat transfer coefficient h_{FS} which is valid for stationary processes only. The symbol * means the convolution integral operator so that in fact the whole past is taken into account.

(AII-3) is an integro-differential equation which would not be very useful if the convolution integral could not be prepared in a suitable way for analog treatment.

The usual way to transform $\varphi(s)$ back is to determine the poles s_n of $\varphi(s)$, to develop $\varphi(s)$ in a partial fraction series

$$\varphi(s) = a_o + \sum_{n=1}^{\infty} \frac{a_n}{s - s_n} , \qquad \text{(AII-4)}$$

where the a_n are the residues in the poles s_n, and then to retransform term by term.

For our problem with boundary condition (3.1.-3), $\varphi(s)$ is a meromorphic function so that the inverse transformation

is possible. G(t) is found as an infinite series of exponentials. After an integration by parts and exchanging sum and integral, one gets the following expression for (AII-3) where we have, for precision reasons, introduced the deviation $\Delta\bar{T}_F(t) = \bar{T}_F(t) - \bar{T}_F^o$ as new dependent variable:

$$\frac{d}{dt}\,\Delta\bar{T}_F = \frac{a_F}{k_F}\left[W^o P(t) - W_L(t)\right]. \qquad \text{(AII-5)}$$

$W^o P(t) = W(t)$ is introduced in order to find again our normalized power function P(t) from the kinetics part; W^o is the reference specific power per unit volume.

$W_L(t)$, the leaking power, is found to be

$$W_L(t) = \frac{8k_F}{(1+p)R_F^2}\left\{\left[\Delta\bar{T}_F(t) - \Delta T_S(t) + \bar{T}_F^o - T_S^o\right] - \sum_{n=1}^{\infty}\alpha_n \Gamma_n(t)\right\} \qquad \text{(AII-6)}$$

with

$$\alpha_n = \frac{1}{2}\,\frac{1+p}{1+p+\left(\frac{p}{4}\right)^2\rho_n^2} \qquad n = 1,\ldots,\infty\,. \qquad \text{(AII-7)}$$

p is the dimensionless quantity

$$p = \frac{4k_F}{h_{FS}R_F}\,, \qquad \text{(AII-8)}$$

which corresponds to 4/Nu in usual notation (Nu = NUSSELT's number). The heat transfer coefficient h_{FS} between fuel and

cladding is for cylindrical geometry:

$$h_{FS} = \frac{1}{R_F} \frac{1}{\frac{1}{k_G} \ln \frac{R_F + \delta_G}{R_F} + \frac{1}{k_S} \ln \frac{R_F + \delta_G + \delta_S}{R_F + \delta_G}} \quad . \qquad \text{(AII-9)}$$

The model for this is a sequence of concentric layers of fuel, of a gap, filled with some material, and of a steel-cladding, with respective heat conductivities k and thicknesses δ.

The ρ_n are the roots of the transcendental equation

$$\rho J_o(\rho) - 2(1 - \frac{p}{8} \rho^2) J_1(\rho) = 0 \ , \qquad \text{(AII-10)}$$

numbered in ascendent order. All ρ_n are positive. The BESSEL functions come from the assumption of cylinder geometry; similar transcendental equations could be found for other geometries. Since p is a known parameter of the system, the roots ρ_n are also known quantities. They have in fact been digitally calculated in advance for a large number of p-values.

The auxiliary functions $\Gamma_n(t)$ (dimension: temperature) are

$$\Gamma_n(t) = e^{-s_n t} \int_0^t \frac{d}{dx} \left[\overline{T}_F(x) - T_S(x) \right] e^{s_n x} dx \qquad n = 1,\ldots,\infty \qquad \text{(AII-11)}$$

where the s_n are just the poles of $\varphi(s)$, occuring in (AII-4), which are related with the ρ_n by

$$s_n = \frac{a_F}{R_F^2}\,\rho_n^2 \qquad n = 1,\ldots,\infty \,. \tag{AII-12}$$

The expressions (AII-11) represent the remainder of the convolution integral of (AII-3), which, at first sight, would much trouble the analog computability of $\overline{T}_F(t)$. Fortunately, the $\Gamma_n(t)$ can easily be generated by solving the equations

$$\frac{d\Gamma_n(t)}{dt} + s_n\Gamma_n(t) = \frac{d}{dt}\left[\overline{T}_F(t) - T_S(t)\right] \qquad n = 1,\ldots,\infty \,. \tag{AII-13}$$

This can be done by the computer itself. The righthand inhomogenous parts are furnished from the main system, where the temperature derivatives are anyhow on hand.

(AII-11) shows that the initial conditions should be $\Gamma_n(0) = 0$. As long as both temperatures $\overline{T}_F(t)$ and $T_S(t)$ do not change with time (steady state), all $\Gamma_n(t)$ are identically zero.

Since $\lim s_n = \infty$, the auxiliary functions vanish identically for very large index n:

$$\lim_{n\to\infty} \Gamma_n(t) = 0 \,, \tag{AII-14}$$

if the inhomogeneous parts are bounded, as it is the case for a significant physical system. The sum in equation (AII-6) converges, since the parameter p is always in the order of unity, or less. Of course, the larger are the temperature derivatives, the worse is the convergence of the process. It should be mentioned that in (AII-6) the term in square brackets can be called the "stationary part" of the

heat transfer, whereas the infinite sum gives the "non-stationary supplement". The notation is a bit different from the usual one also for the stationary case, because we set the heat transfer term proportional to the difference of mean fuel temperature and $\bar{T}_S$, and not to that between surface temperature and $\bar{T}_S$.

Numerical values of all coefficients are compiled in paragraph 3.4.

APPENDIX III

Coolant heat balance with slug flow model

Whereas for "normal" liquids the PRANDTL number $Pr = \nu_C/a_C$ (ν = kinematic viscosity) is in the order of unity, it is only about 10^{-2} for liquid metals. This means that the geometrical similarity between velocity profile and temperature profile in a tube is disturbed. The former shows a sharp jump near the wall to a nearly constant value inside the turbulent flow. The temperature, however, is practically not influenced by turbulent mixture and shows thus the same profile as in a solid body which, e.g., is parabolic for a circular cylinder. For other geometries one finds another shape so that the concept of equivalent diameters (of differently shaped tubes) breaks down. Moreover, no REYNOLDS number can be found in default of a generally valid characteristic length, and thus no universal heat transfer coefficient exists. Only, for a well-defined specific geometry, some replacing non-transferable value can be calculated from the known stationary temperature distribution.

For this case, the so-called "slug flow model" has been conceived [7]. The radial heat transport in the coolant is assumed to be performed by the conductivity k_C only, like in a metallic slug which is, however, moving along its axis with constant velocity. The velocity profile is considered to be entirely flat which is not too bad an assumption for turbulent flow. Axial heat conduction is again neglected.

The SORA core is composed by a number of parallel circular-cylindrical fuel rods, touching mutually and forming a bundle of hexagonal pattern. The interspaces between the

rods are the coolant channels. The neutral fibres of the coolant spandrels form just the circumscribing hexagonal cylinder of each rod.

In order to simplify the geometry, we reduce the difference space between hexagon and circle to a circular ring of equal area. The channel "thickness" is averaged in this way and any azimuthal dependency is eliminated. For the same power output the necessary mean coolant velocity is conserved. This procedure is somewhat criticizable, especially in the light of what we have said above [1]. There is, however, no other way in practice to overcome the mathematical difficulties.

We assume that the heat leaking to the reflector (or blanket) is negligible against the one carried away by the coolant. Then the balance for the annular coolant volume is:

$$\frac{1}{a_C}\,\frac{DT_C(r,t)}{Dt} = \frac{\partial^2 T_C(r,t)}{\partial r^2} + \frac{1}{r}\,\frac{\partial T_C(r,t)}{\partial r} \quad . \qquad \text{(AIII-1)}$$

T_C is the temperature of the coolant and $a_C = k_C/\rho_C c_C$ is its thermal diffusivity. An internal (volumetric) source does not exist.

Let us label the inner and outer radii of the coolant annulus R_i and R_a, respectively. The boundary conditions are

$$\left.\frac{\partial T_C(r,t)}{\partial r}\right|_{r=R_a} = 0 \qquad \text{insulation at the neutral fibre} \qquad \text{(AIII-2)}$$

---

1) Seeing later on that the coolant temperature feedback is anyhow very small one may be composed.

$$k_C \cdot \frac{\partial T_C(r,t)}{\partial r}\bigg|_{r=R_i} = h_{SC}\left[T_S(t) - \bar{T}_C(t)\right] \quad \text{heat inflow.} \tag{AIII-3}$$

This condition can also be written as

$$k_C \int_{V_C} \text{div grad } T_C(r,t)dV = 2\pi R_i \, L \, h_{SC}\left[T_S(t) - \bar{T}_C(t)\right] \tag{AIII-4}$$

which is a convenient form for later on. The identity of conditions (AIII-3) and (AIII-4) can easily be seen when transforming the volume integral in a surface integral and integrating, taking into account the insulation condition (AIII-2). L means the active coolant channel length. Furthermore, we identify the reference temperature $\bar{T}_C(t)$ of the preceding paragraph with the mean coolant temperature

$$\bar{T}_C(t) = \frac{2}{R_a^2 - R_i^2} \int_{R_i}^{R_a} T_C(r,t)\, r\, dr \,. \tag{AIII-5}$$

The total or "substantial" differential operator D/Dt means

$$\frac{D}{Dt} = \frac{\partial}{\partial t} + (\vec{v} \cdot \text{grad}). \tag{AIII-6}$$

In the SORA case, the velocity vector $\vec{v}$ has only a z-component w along the channel direction so that we have

$$\frac{DT_C(\vec{r},t)}{Dt} = \frac{\partial T_C(\vec{r},t)}{\partial t} + w\,\frac{\partial T_C(\vec{r},t)}{\partial z} \,. \tag{AIII-7}$$

Strictly spoken, T_C is of course also a function of z, since the coolant must be heated up in the presence of a source. We assume, however, but only at this point, the temperature increase to be linear so that $\partial T_C/\partial z$ is a constant, or more precisely, a pure time function, also practically independent of r. At the same time $\partial^2 T_C/\partial z^2 = 0$, and the respective term in the LAPLACE operator (already omitted in (AIII-1)) vanishes truly. The linear increase is correct only if the heat generation along the axial direction is uniform, thus with z-independent neutron flux. This assumption is not very bad for a small core with a relatively large reflector; all this in accordance with our point reactor model assumption.

We disregard any hydraulic inlet distance which has little importance in our case of pure heat conduction.

The velocity w is produced by the pressure head from the coolant pump. Only forced convection is considered, since otherwise, with natural convection, w would itself be a system variable, reinfluenced by the coolant temperature distribution of the whole circuit. Then the perturbation variable should be outside of this circuit, say a secondary or tertiary mass flow. We should then describe and simulate also the heat exchanger. Due to its large time constants, such a control is by far too sluggish for the very sensitive SORA dynamics so that a previously discussed idea of natural convection can, without doubt, be rejected already by these qualitative considerations.

Now, the velocity w is fixed by the condition that the mean power $\pi R_F^2 L W^o$ of a fuel element should just be carried away. Let δT_C^o be the wanted heating span from inlet to outlet, then

$$\pi(R_a^2 - R_i^2)\, w\, \frac{k_C}{a_C}\, \delta T_C^o = \pi R_L^2 L\, W^o, \qquad \text{(AIII-8)}$$

hence

$$w = \frac{R_F^2 L}{R_a^2 - R_l^2} \frac{a_C W^o}{k_C \delta T_C^o} \quad ^{1)}. \qquad \text{(AIII-9)}$$

w can be a perturbation variable. However, with respect to the fast reactivity pulsation, all possible w-changes are slow, also in an emergency case. Thus, for the simulation, simple steps on w are forbidden.

The time function $\partial T_C(\vec{r},t)/\partial z$ is, for a linear z-increase of temperature,

$$\frac{\partial T_C(\vec{r},t)}{\partial z} = \frac{\overline{T}_C^{out}(t) - T_C^{in}}{L} = \frac{\overline{T}_C(t) - T_C^{in}}{L/2} \qquad \text{(AIII-10)}$$

where the bar means always the average in r-direction. To eliminate the outlet temperature, the difference quotient can also be taken between mean coolant temperature, which appears just at half the channel length, and the constant inlet temperature.

The inlet temperature, too, can be considered as a perturbation quantity like w, and with similar restrictions.

Introducing all these expressions into (AIII-1), we get:

$$\frac{1}{a_C} \frac{\partial T_C(r,t)}{\partial t} = \frac{\partial^2 T_C(r,t)}{\partial r^2} + \frac{1}{r} \frac{\partial T_C(r,t)}{\partial r} - \frac{2w}{a_C L} \left[\overline{T}_C(t) - T_C^{in} \right]. \qquad \text{(AIII-11)}$$

---

1) This expression is of course consistent with (AIII-3) and can replace it in steady state.

Now, we average this equation over the volume, term by term:

$$\frac{1}{a_C}\left\{\frac{d\bar{T}_C(t)}{dt}+\frac{2w}{L}\left[\bar{T}_C(t)-T_C^{in}\right]\right\}=\frac{1}{V_C}\int_{V_C}\left[\frac{\partial^2 T_C(r,t)}{\partial r^2}+\frac{1}{r}\frac{\partial T_C(r,t)}{dr}\right]dV. \tag{AIII-12}$$

The integrand of the right hand side is just div grad $T_C(r,t)$ so that, by applying the boundary condition (AIII-4), results

$$\frac{d}{dt}\Delta\bar{T}_C(t)=\frac{a_C}{k_C}\frac{2R_i}{R_a^2-R_i^2}h_{SC}\left[\Delta T_S(t)-\Delta\bar{T}_C(t)+T_S^o-\bar{T}_C^o\right]-$$

$$-\frac{2w}{L}\left[\Delta\bar{T}_C(t)+T_C^o-T_C^{in}\right]. \tag{AIII-13}$$

In this manner we have found an ordinary differential equation for the mean coolant temperature $\bar{T}_C(t)$ [1]. Our system of thermal equations is thus closed.

Nevertheless, we must not forget that this is only owing to the fact of having introduced just $\bar{T}_C(t)$ as the reference temperature in the cladding equation, and no other one. We have to purchase this ease with the assumption of a "heat transfer coefficient" h_{SC} in the boundary condition (AIII-3).

It must be established that in this way any time constant between surface and mean temperature of the coolant is neglected. However, we have done this also for the gap and cladding layers. The neglection is also in accordance with the other necessary assumption made, namely that the axial

---

[1]) This equation is well-known for normal convectional heat transfer. The existence of an equation of the same type must, however, be proved here.

temperature slope $\partial T_C/\partial z$ is independent of r for each t.

In the case of SORA, these approximations are perhaps not always very good. Nevertheless, for dynamic purposes, we need only a sufficiently good picture of the mean temperatures with their time behaviour. On account of our geometrical deformation of the coolant channel the true spatial distribution of temperature can anyhow not be calculated. It can be taken for granted that the uncertainty in the mean coolant temperature is by far lower than the uncertainty in the corresponding temperature coefficients so that any further expenditure is not worth the effort.

Thus we take the heat transfer coefficient h_{SC} from the steady temperature distribution, applying again the slug flow model. It should have such a value that it provides just the difference between surface and mean coolant temperatures in the steady reference state.

The idea is to calculate the difference between the coolant temperature at the inner ("heat inflow") surface and the mean coolant temperature in steady conditions. Then h_{SC} is obtained from a relation like

$$h_{SC} = \frac{W^o \cdot V_F}{F_{SC}[T_C(R_i) - T_C]} , \qquad \text{(AIII-14)}$$

where $W^o V_F$ is the total heat production in a fuel rod and F_{SC} is a properly chosen exchange surface. In this way, the radial temperature drop in the coolant is thought to be produced by a stagnant layer of NaK, but with a certain correction coefficient, as we shall see.

Equation (AIII-11) reads in steady state

$$\frac{d^2T_C(r)}{dr^2} + \frac{1}{r}\frac{dT_C(r)}{dr} - \frac{2w}{a_C L}(\bar{T}_C - T_C^{in}) = 0, \qquad \text{(AIII-15)}$$

or by using (AIII-9)

$$\frac{d^2T_C(r)}{dr^2} + \frac{1}{r}\frac{dT_C(r)}{dr} - \frac{R_F^2}{R_a^2 - R_i^2}\frac{W^o}{k_C} = 0. \qquad \text{(AIII-16)}$$

If we abbreviate

$$\frac{R_F^2}{R_a^2 - R_i^2} = \xi \qquad \text{(AIII-17)}$$

and apply the two boundary conditions (AIII-2) and (AIII-3) for the steady state, where

$$h_{SC}\left[T_S^o - \bar{T}_C^o\right] = \frac{R_F^2}{2R_i} W^o, \qquad \text{(AIII-18)}$$

the solution is

$$T_C(r) = \frac{\xi}{2}\frac{W^o}{k_C}\left(\frac{r^2}{2} - R_a^2 \ln\frac{r}{R_a}\right). \quad ^{1)} \qquad \text{(AIII-19)}$$

Let us abbreviate the ratios of radii

$$\frac{R_i}{R_a} = q \qquad \frac{r}{R_a} = x. \qquad \text{(AIII-20)}$$

Then

$$T_C(r) = \frac{\xi}{2}\frac{W^o}{k_C} R_a^2\left(\frac{x^2}{2} - \ln x\right), \qquad \text{(AIII-21)}$$

---

1) An arbitrary additive constant, determining the absolute temperature level, is omitted.

$$T_C(R_i) = \frac{\xi}{2} \frac{W^o}{k_C} R_a^2 \left(\frac{q^2}{2} - \ln q \right) , \qquad \text{(AIII-22)}$$

$$\bar{T}_C = \frac{2}{R_a^2 - R_i^2} \int_{R_i}^{R_a} T_C(r)\, r\, dr = \frac{\xi}{2} \frac{W^o}{k_C} R_a^2 \left(\frac{1+q^2}{4} + \frac{1}{2} + \frac{q^2}{1-q^2} \ln q \right) , \qquad \text{(AIII-23)}$$

$$T_C(R_i) - \bar{T}_C = \frac{\xi}{2} \frac{W^o}{k_C} R_a^2 \left(\frac{q^2 - 3}{4} - \frac{\ln q}{1-q^2} \right) . \qquad \text{(AIII-24)}$$

Let us now determine the "mean radius" $\bar{R}$, where the mean temperature $\bar{T}_C = T_C(\bar{R})$ is just reached.

If we label

$$\frac{\bar{R}}{R_a} = \eta , \qquad \text{(AIII-25)}$$

we have simply from (AIII-21)

$$T_C(\bar{R}) = \frac{\xi}{2} \frac{W^o}{k_C} R_a^2 \left(\frac{\eta^2}{2} - \ln \eta \right) . \qquad \text{(AIII-26)}$$

By equating (AIII-26) and (AIII-23) we get

$$\frac{\eta^2}{2} - \ln \eta = \frac{1+q^2}{4} + \frac{1}{2} + \frac{q^2}{1-q^2} \ln q . \qquad \text{(AIII-27)}$$

This transcendental equation cannot be solved for η in general terms of q. Fortunately, we know the exact value of q, which is

$$q = \sqrt{\pi/2\sqrt{3}} = 0{,}9523128065 .$$

The right hand side of (AIII-27) is +0,5007575577 so that η can be determined by trial:

$$\eta = 0,97260263.$$

The appropriate expression of F_{SC} for a hollow cylinder is:

$$F_{SC} = 2\pi L \frac{\bar{R} - R_i}{\ln (\bar{R}/R_i)} = 2\pi L R_a \frac{\eta - q}{\ln \eta/q} . \qquad \text{(AIII-28)}$$

By inserting $\eta = \bar{R}/R_a$, it follows:

$$F_{SC} = 2\pi L R_a \cdot 0,96241496. \qquad \text{(AIII-29)}$$

Finally, with $V_F = \pi R_F^2 L$, and by introducing (AIII-17), (AIII-24), and (AIII-29) into (AIII-14), we get

$$h_{SC} = \frac{k_C}{R_a} \frac{(1 - q^2) \ln \eta/q}{(\eta - q)\left(\frac{q^2 - 3}{4} \quad \frac{\ln q}{1 - q^2}\right)} = \frac{k_C}{R_a} \cdot 51,222023. \qquad \text{(AIII-30)}$$

Note that, with the slug flow model, the "heat transfer coefficient" h_{SC} is independent of the velocity w.

Once more, it should be emphasized that neither the method nor the value given here is transferable to other geometries of the coolant channel.

Bibliography

[1] ASAOKA, T., MISENTA, R. — Two-Neutron-Group Kinetic Theory and Calculations for a Fast Reactor Periodically Pulsed by Reactivity Variations; report EUR 2217.e (1965)

[2] ASAOKA, T., MISENTA, R. — Kinetic Theory and Calculations in a Few-Energy-Group Two-Space-Point Model for a Fast Reactor Periodically Pulsed by Reactivity Variations; report EUR 2273.e (1965)

[3] SCHWALM, D. — On a Multigroup Kinetics; report EUR 2285.e (1965)

[4] BLÄSSER, G., MISENTA, R., RAIEVSKI, V. — The Kinetic Theory of a Fast Reactor Periodically Pulsed by Reactivity Variations; report EUR 493.e (1964)

[5] STIEVENAERT, M. — Etude des Charactéristiques d'un Réacteur à Impulsion; report Belgonucléaire BN 6203-25 (1962)

[6] PALINSKI, R. — Lösung der instationären Wärmeleitungsgleichung mit zeitabhängiger Umgebungstemperatur und räumlich ungleichmäßig verteilter Wärmequelle; Nukleonik 6, 289-303 (1964) and report EUR 1089.d (1965)

[7] HALL, W.B.
Reactor heat transfer;
Nuclear Engineering Monographs, Temple Press Ltd., London (1961)

[8] CALIGIURI, G.P.
Sull' utilizzazione con calcolatore analogico del principio del massimo per l'ottimizzazione d'un sistema idro-termo-elettrico;
Rivista "CALCOLO", to appear (1965)

[9] Van WAUWE, A.
The SIOUX system;
report EUR 1917.e (1964)

[10] De BACKER, W., Van WAUWE, A.
The SIOUX System and Hybrid Block Diagrams, Simulation;
to appear (1965)

[11] DEL BIGIO, G., d'HOOP, H.
Analog Programming and Checking (APACHE I);
report EUR 189.f (1963)

[12] BECKER, W., DE LOTTO, I.
Pattern Display Considerations for a Programming Aid Machine Linking a Digital and an Analog Computer;
report EUR 410.e (1965)

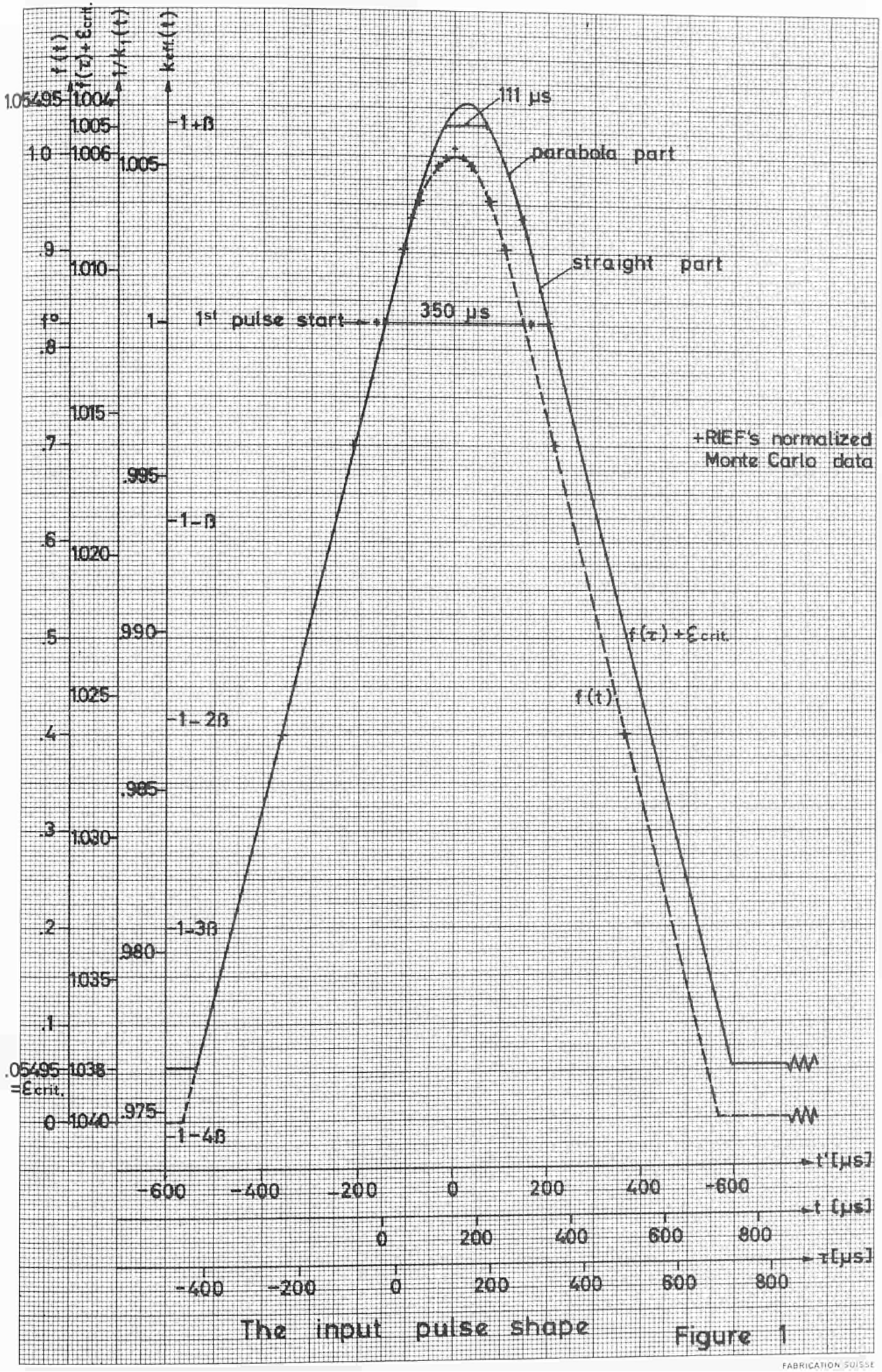

The input pulse shape Figure 1

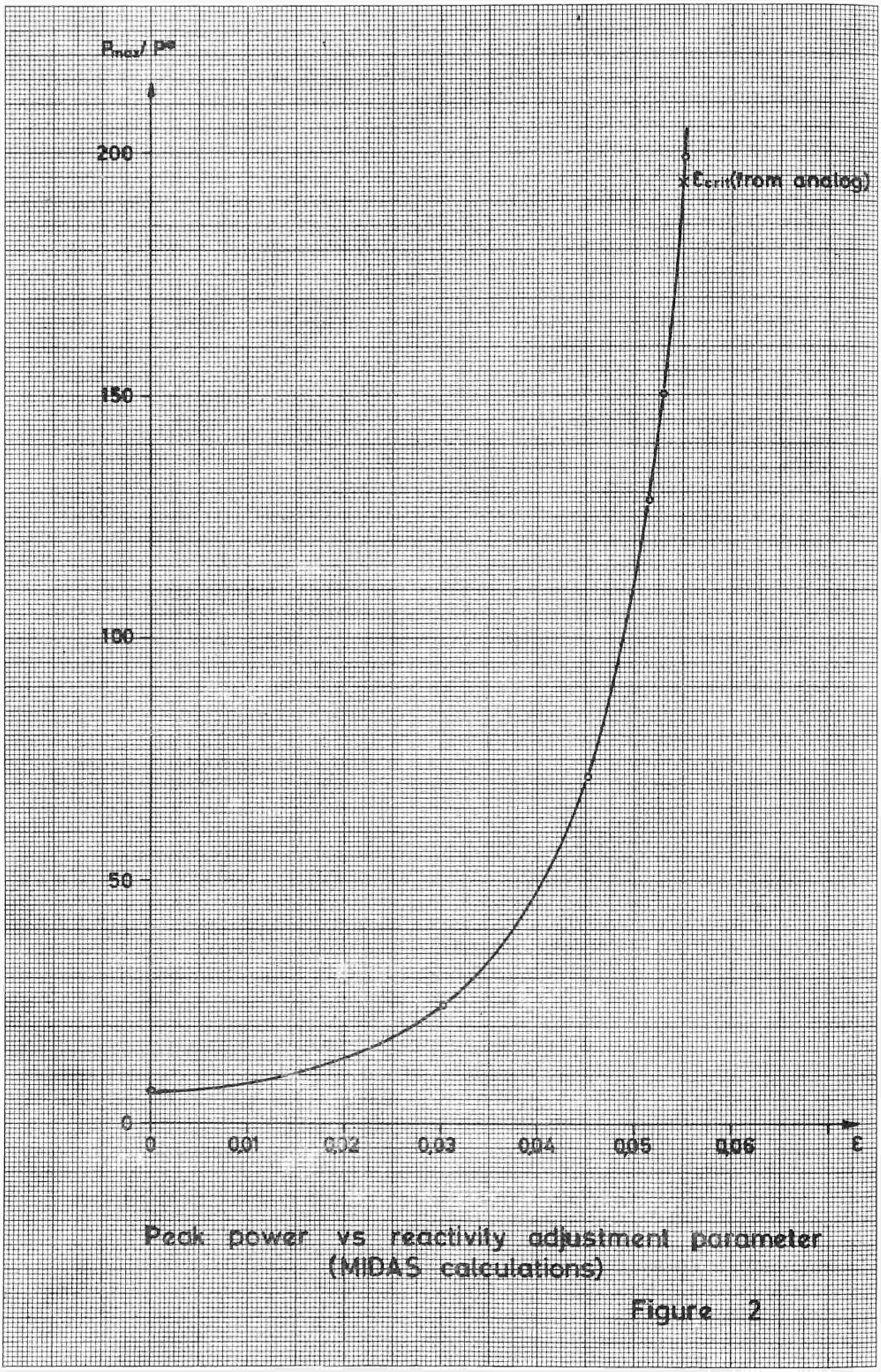

Peak power vs reactivity adjustment parameter (MIDAS calculations)

Figure 2

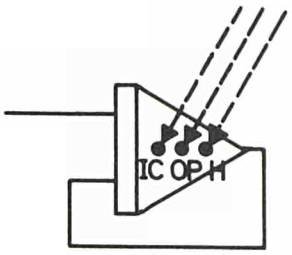

a) "group„

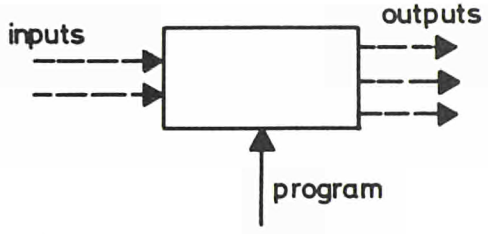

b) " command program„

Elements of hybride block diagrams

Figure 3

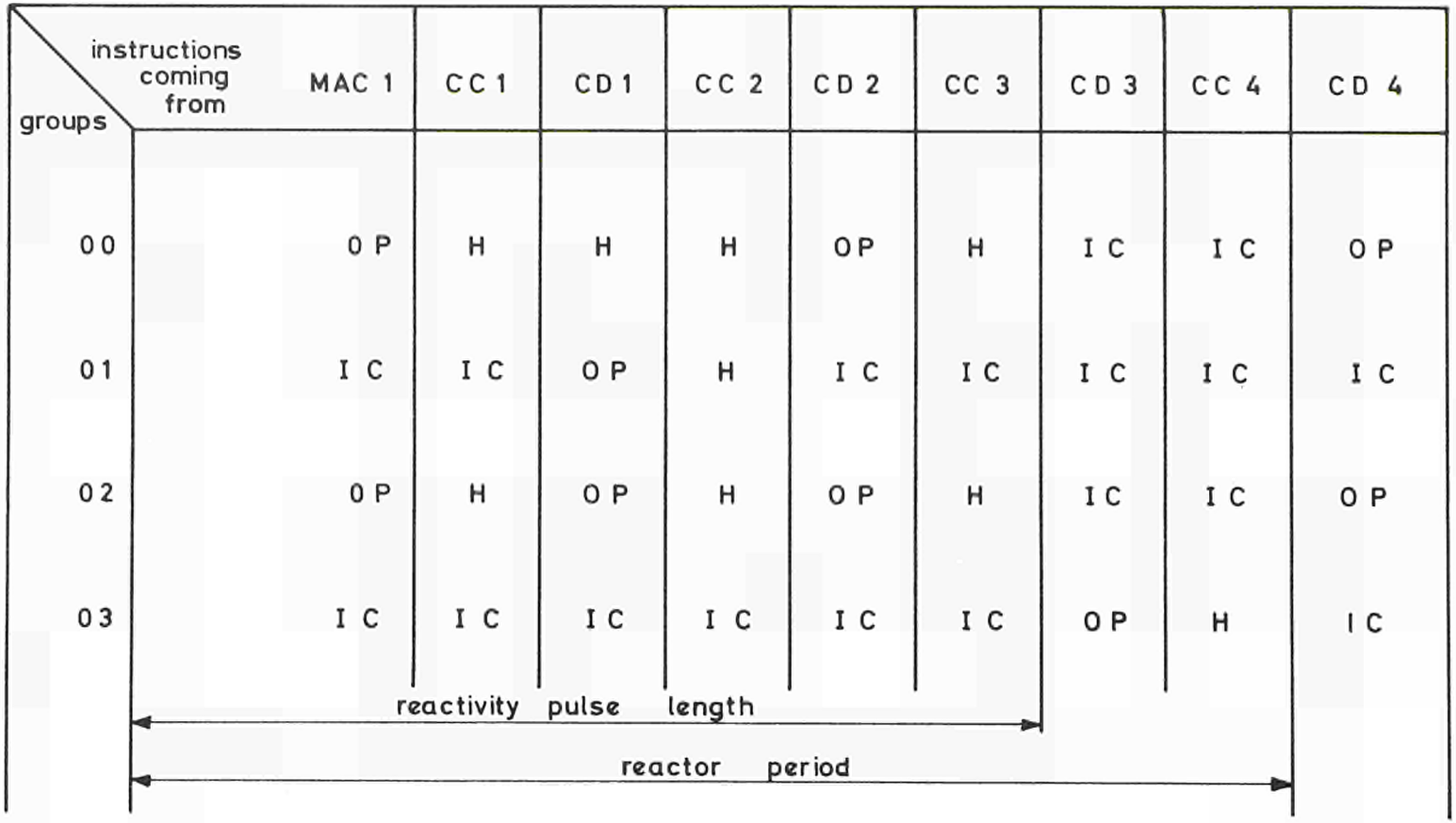

Sequence of modes

Figure 4

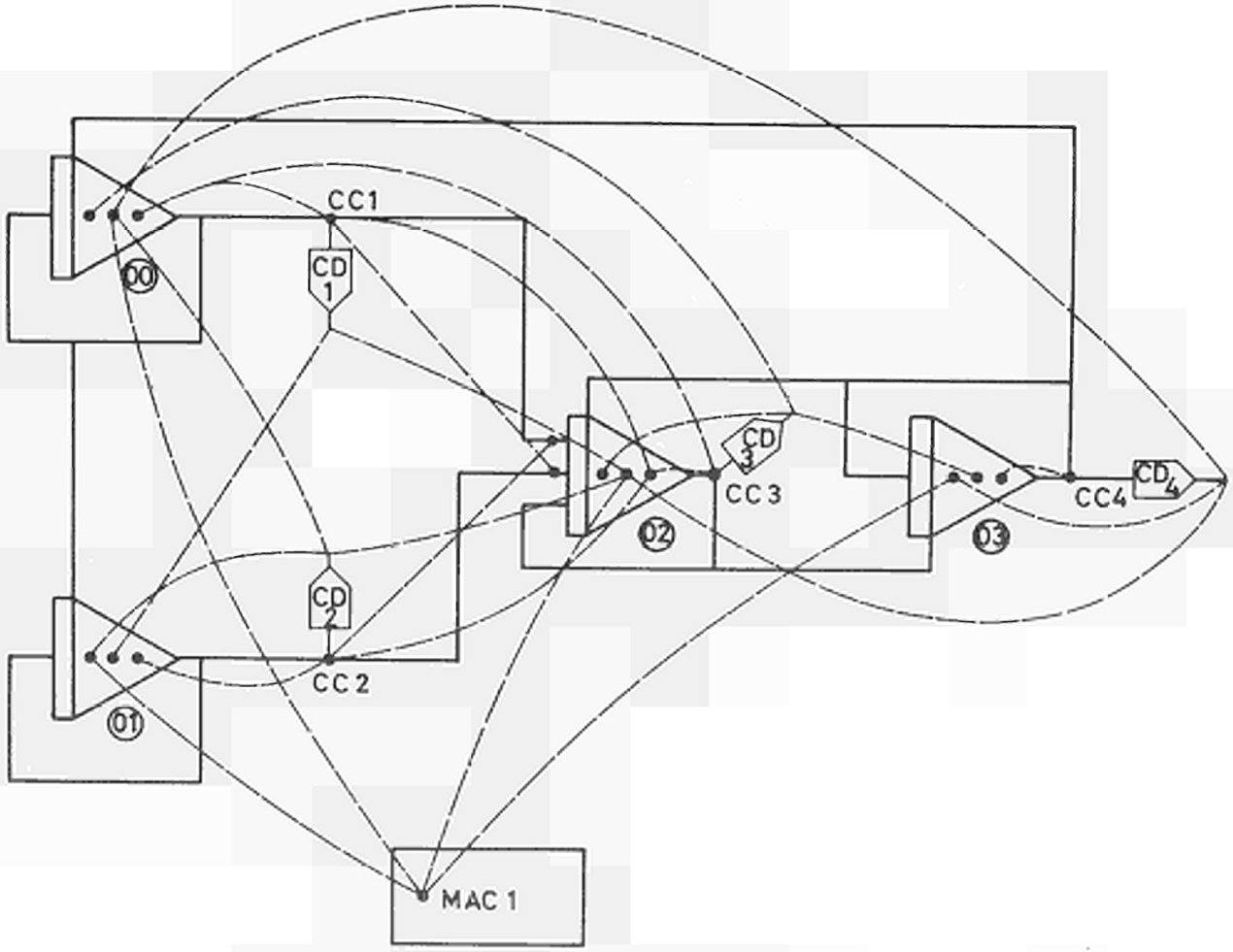

The hybride block diagram

Figure 5

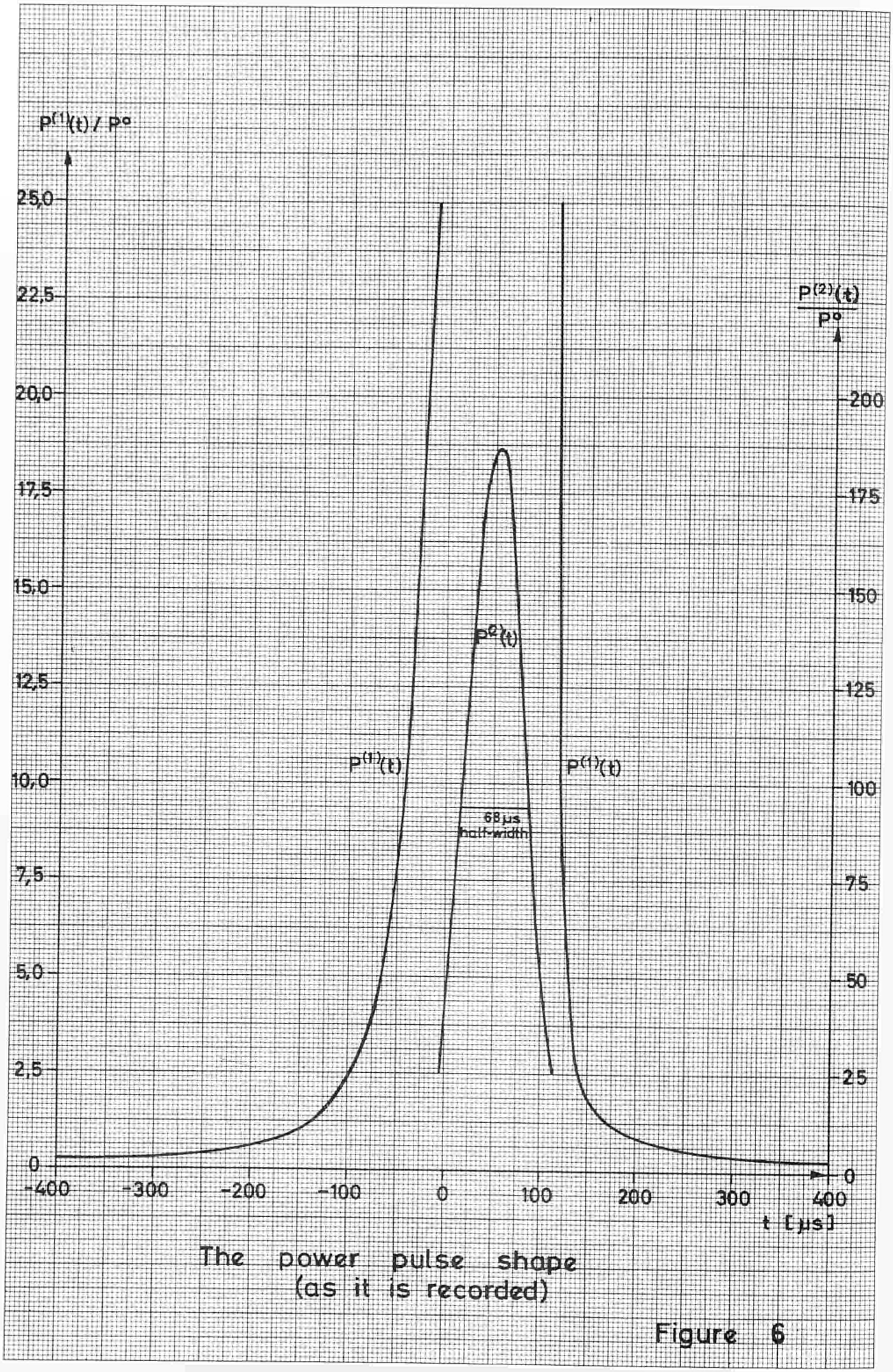

The power pulse shape
(as it is recorded)

Figure 6

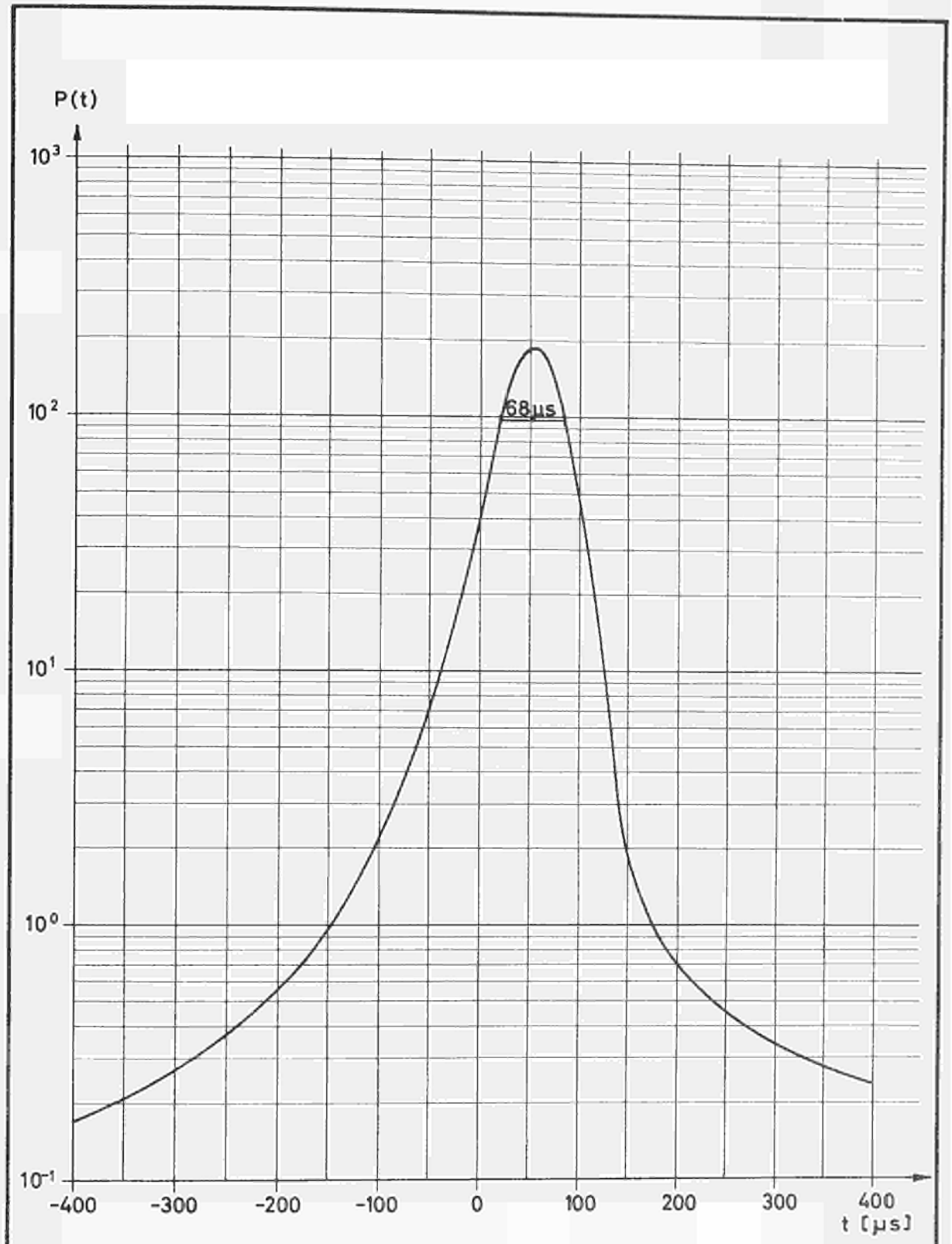

The power pulse shape
(logarithmic scale)

Figure 7

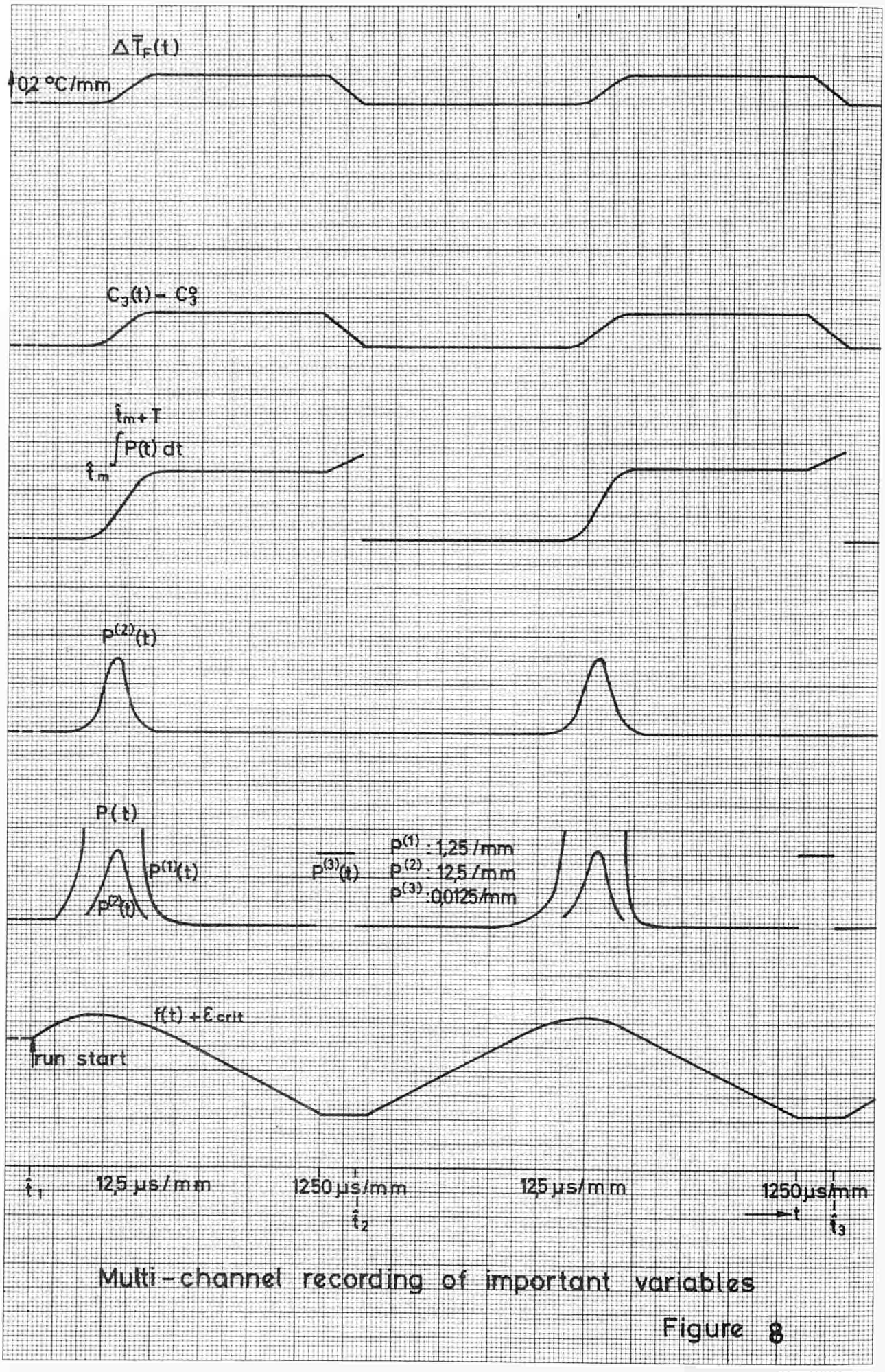

Multi-channel recording of important variables

Figure 8

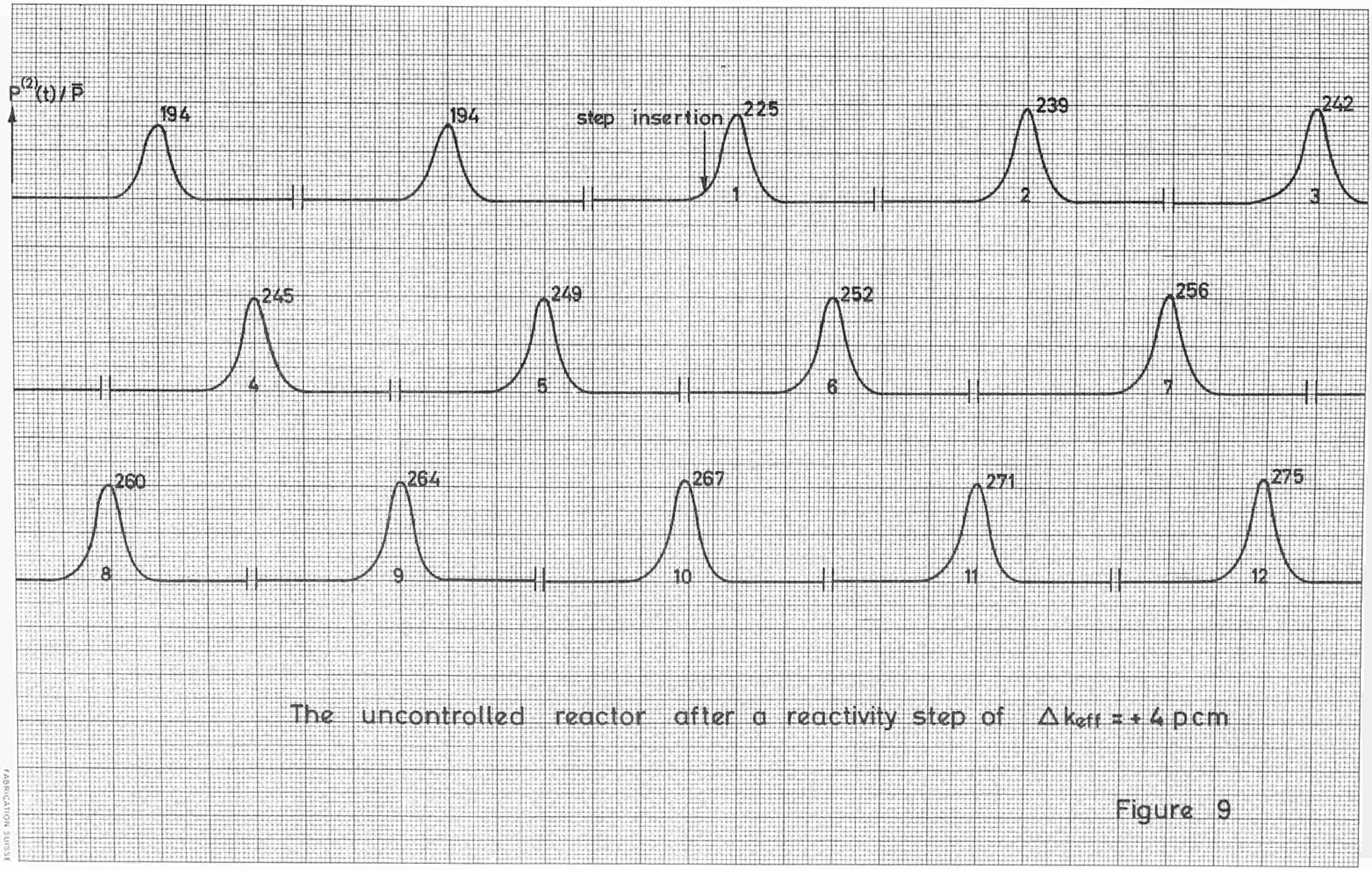

The uncontrolled reactor after a reactivity step of $\Delta k_{eff} = +4$ pcm

Figure 9

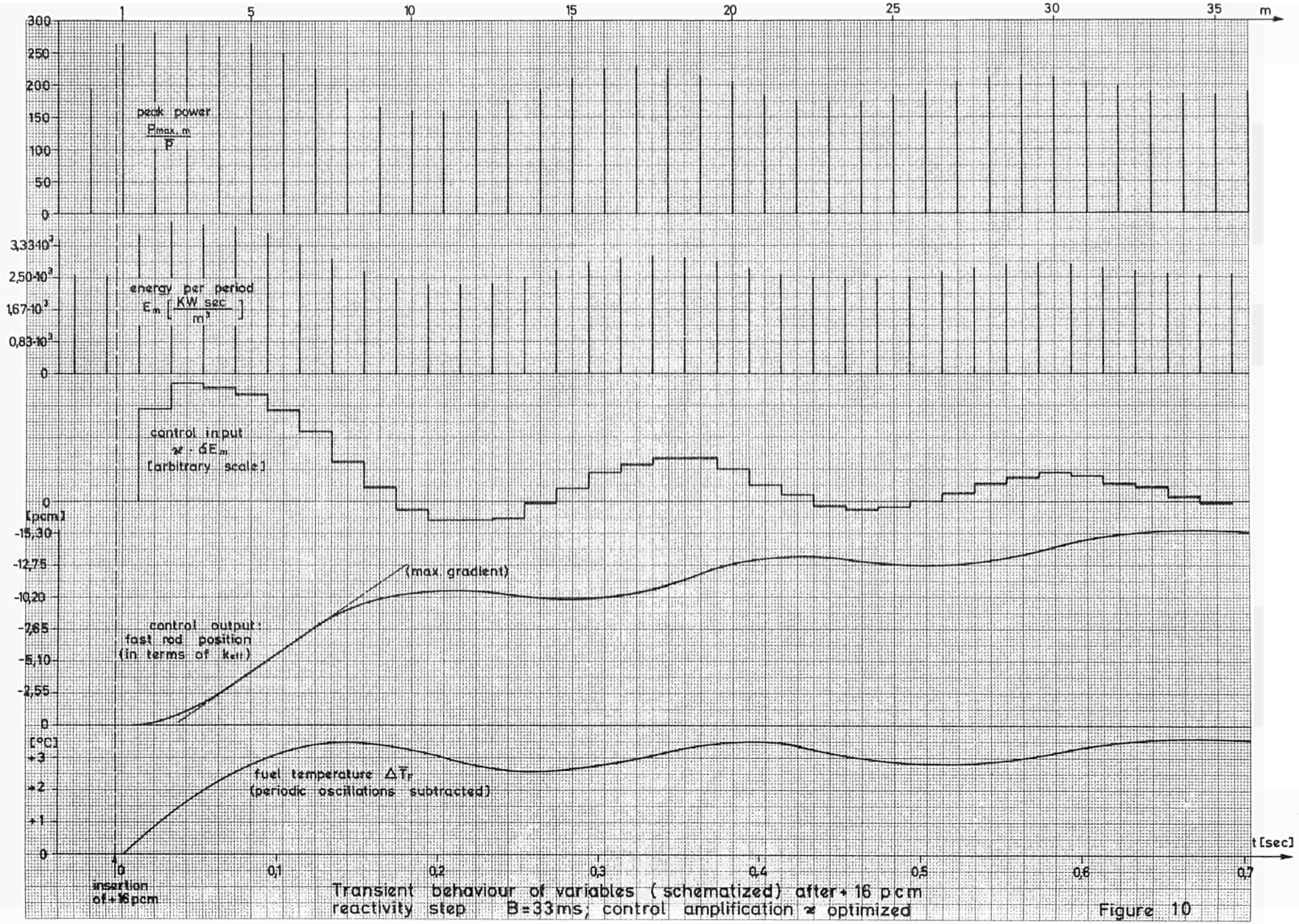

Transient behaviour of variables (schematized) after + 16 p c m reactivity step B=33ms; control amplification ∝ optimized

Figure 10

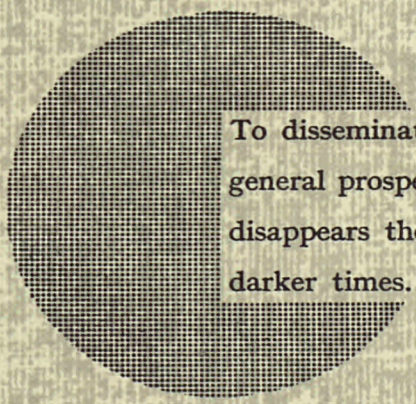

To disseminate knowledge is to disseminate prosperity — I mean general prosperity and not individual riches — and with prosperity disappears the greater part of the evil which is our heritage from darker times.

Alfred Nobel

SALES OFFICES

All Euratom reports are on sale at the offices listed below, at the prices given on the back of the cover (when ordering, specify clearly the EUR number and the title of the report, which are shown on the cover).

PRESSES ACADEMIQUES EUROPEENNES
98, Chaussée de Charleroi, Bruxelles 6

Banque de la Société Générale - Bruxelles
compte N° 964.558,
Banque Belgo Congolaise - Bruxelles
compte N° 2444.141,
Compte chèque postal - Bruxelles - N° 167.37,
Belgian American Bank and Trust Company - New York
compte No. 22.186,
Lloyds Bank (Europe) Ltd. - 10 Moorgate, London E.C.2,
Postcheckkonto - Köln - Nr. 160.861.

OFFICE CENTRAL DE VENTE DES PUBLICATIONS DES COMMUNAUTES EUROPEENNES
2, place de Metz, Luxembourg (Compte chèque postal N° 191-90)

BELGIQUE — BELGIË
MONITEUR BELGE
40-42, rue de Louvain - Bruxelles
BELGISCH STAATSBLAD
Leuvenseweg 40-42 - Brussel

DEUTSCHLAND
BUNDESANZEIGER
Postfach - Köln 1

FRANCE
SERVICE DE VENTE EN FRANCE
DES PUBLICATIONS DES
COMMUNAUTES EUROPEENNES
26, rue Desaix - Paris 15e

GRAND-DUCHE DE LUXEMBOURG
OFFICE CENTRAL DE VENTE
DES PUBLICATIONS DES
COMMUNAUTES EUROPEENNES
9, rue Goethe - Luxembourg

ITALIA
LIBRERIA DELLO STATO
Piazza G. Verdi, 10 - Roma

NEDERLAND
STAATSDRUKKERIJ
Christoffel Plantijnstraat - Den Haag

EURATOM — C.I.D.
51 - 53, rue Belliard
Bruxelles (Belgique)